Progress in Reaction Kinetics and Mechanism

ARTICLE

Open Access

https://doi.org/10.48130/prkm-0026-0006

Progress in Reaction Kinetics and Mechanism **2026**, 51: e014

Exploring reaction mechanism for ammonia combustion: reactive molecular dynamics simulations and kinetic modeling study

Shuhao Li[1*], Kunqi Wang[2*], Licheng Zhong[1], Shuanghui Xi[3*], Zhikun Cao[1], Xiao Guo[1], Junxing Hou[4] and Zhenhua Wen[1]

[1] *School of Aero Engine, Zhengzhou University of Aeronautics, Zhengzhou 450046, China*
[2] *Aero Engine Corporation of China (AECC) Chengdu Engine Company Ltd., Chengdu 610503, China*
[3] *School of Mechanical Engineering, Zhengzhou University of Aeronautics, Zhengzhou 450046, China*
[4] *School of Aerospace Engineering, Zhengzhou University of Aeronautics, Zhengzhou 450046, China*
* Correspondence: lish@zua.edu.cn (Li S); wkq0213@163.com (Wang K); xishuanghui@zua.edu.cn (Xi S)

Abstract

This study employs Reactive force field molecular dynamics (ReaxFF MD) simulations to probe ammonia pyrolysis and oxidation across temperatures and equivalence ratios, revealing accelerated combustion with temperature and key species variations. Based on the analysis of combustion mechanisms through molecular dynamics simulations and reaction pathway analysis derived from six published combustion mechanisms, this study has established a relatively comprehensive combustion pathway for ammonia. A detailed kinetic model for ammonia combustion, comprising 41 species and 351 reactions, is developed using a hierarchical construction method. The model demonstrated excellent agreement with a wide range of experimental data, including ignition delay times (IDTs), laminar burning velocities (LBVs), and species concentrations under diverse conditions, thereby validating its predictive capability. Reaction path analysis and sensitivity analysis revealed that the ammonia combustion process involves two major pathways: N_2 generation and NO_x generation from NH_2. Key reactions affecting performance include NH_3, NH_2, NH, and H. The reaction $NH_2 + NO = N_2 + H_2O$ exhibits the most significant inhibiting effect on ammonia combustion. Meanwhile, $H + O_2 = O + OH$ remains a strong promoter for LBVs and key species formation in ammonia, whereas its promoting effect on ammonia ignition performance becomes considerably weaker. In contrast, the reaction $NH_2 + HO_2 = H_2NO + OH$ shows the strongest promoting influence on IDTs. Additionally, NH_2-involved reactions that generate radicals such as OH and O, as well as those yielding N_2 and H_2O, also substantially enhance the ignition performance of ammonia.

Citation: Li S, Wang K, Zhong L, Xi S, Cao Z, et al. 2026. Exploring reaction mechanism for ammonia combustion: reactive molecular dynamics simulations and kinetic modeling study. *Progress in Reaction Kinetics and Mechanism* 51: e014 https://doi.org/10.48130/prkm-0026-0006

Introduction

The overexploitation of fossil fuels has triggered severe resource depletion and environmental crises, particularly through excessive CO_2 emissions[1]. This urgency drives the global energy transition toward low-carbon and carbon-free alternatives to enable sustainable development[2]. Although hydrogen (H_2) is recognized as a promising carbon-neutral energy carrier, its inherent physicochemical limitations pose significant barriers to its safe storage, efficient transportation, and large-scale deployment[1]. Ammonia (NH_3) is an emerging carbon-free fuel that boasts a high hydrogen content and high energy density. Owing to its ease of liquefaction, it offers practical advantages for storage, transportation, and energy storage systems[2]. Its efficient utilization plays an important role in building a low-carbon energy system. Currently, ammonia is widely regarded as a highly promising alternative to fossil fuels, with successful tests in gas turbines and internal combustion engines demonstrating its potential for practical application[3].

However, the utilization of ammonia as a fuel presents obstacles, including its low laminar burning velocity (LBV), poor flammability, and narrow flammability range. As a result, early research mainly focused on co-combustion with highly reactive fuels such as H_2[4], methane (CH_4)[5], or using techniques such as oxy-fuel combustion[6] to improve the reactivity of ammonia. Although there has been some progress in the research on the co-combustion of ammonia and highly reactive fuels, research on the combustion characteristics of pure ammonia in an air atmosphere is still relatively scarce. More importantly, the combustion reaction mechanism of ammonia is not yet fully understood, and key parameters such as pollutant formation are still incomplete, which hinders the large-scale application of ammonia as a fuel[7]. Hence, to enable the effective use of ammonia as an energy source, a deeper understanding of its combustion behavior, characteristics, and underlying reaction mechanisms is required.

As a key combustion parameter, the LBV is essential for describing flame stability, extinction, and structure, while also playing a vital role in the assessment and validation of chemical kinetic models. Takizawa et al.[8] measured the LBV of NH_3/Air mixtures under different equivalence ratios (ϕ) using the spherical vessel (SV) method. They found that the LBV of NH_3 peaked at approximately 7.2 cm/s at an equivalence ratio of 1.1. Furthermore, under lean fuel conditions, the flame front exhibited a concave inward structure, a phenomenon attributed to the buoyancy effect that promotes upward flame propagation. Mei et al.[9] compared the flame morphology and burning velocity of NH_3/Air under normal and oxygen-enriched conditions. Their results demonstrated that an oxygen-enriched environment enhances flame propagation and significantly mitigates the buoyancy effect. Additionally, they observed that while burning velocity increases with oxygen concentration, the primary reaction pathway of NH_3 remains unchanged. Lhuillier et al.[10] employed the spherical flame method to measure the laminar burning velocity of NH_3 under various temperatures and hydrogen concentrations at atmospheric pressure. They reported a progressive increase in LBV with elevated hydrogen content and temperature. Hayakawa et al.[11] were the first to experimentally measure the laminar burning velocity of NH_3/Air at pressures up to 5 atm, reporting a maximum unstretched LBV of approximately

7 cm/s. Chen et al.[12] examined laminar flame parameters of NH_3/Air mixtures under varying equivalence ratios and initial pressures. They noted that the maximum flame velocity occurs at an equivalence ratio of 1.1, and both flame speed and flame thickness decrease with increasing pressure. Shrestha et al.[13] measured ammonia flame velocity under high temperature and pressure with varying hydrogen and oxygen concentrations. Their findings aligned with those of Mei & Lhuillier, confirming that LBV increases with temperature and decreases with pressure. They also provided the first measurements of ammonia burning velocity at 7 and 10 bar. Kanoshima et al.[14] and Liang et al.[15] also investigated NH_3/Air LBV under high temperature and pressure conditions, corroborating the results reported by Shrestha et al. Furthermore, Alvarez et al.[16] studied NH_3/Air flames under high pressure and observed a non-linear decrease in LBV with increasing pressure, identifying reactions involving NH_2 and NO as particularly significant. Zhou et al.[17] measured laminar burning velocities of NH_3/Air, NH_3/H_2/Air, NH_3/CO/Air, and NH_3/CH_4/Air within temperature and equivalence ratio ranges of 298–423 K and 0.7–1.4, respectively, and developed a new chemical mechanism for validation. Kohansal et al.[18] explored NH_3/CH_4/Air flames and found that at an ammonia molar fraction of 0.4, the LBV reached values comparable to those of hydrocarbon flames. They also highlighted the absence of direct competitive reactions between NH_3 and CH_4, noting that competition occurs primarily through consumption of O/H radicals. Liu et al.[19] studied NH_3/C_2H_4/Air flames under elevated temperature and pressure. Their results indicated that C_2H_4 addition promotes the formation of new intermediates, enriches reaction pathways, accelerates consumption of both fuels, and increases ammonia flame velocity. They also emphasized the critical role of the reaction $H + O_2 = OH + O$ in enhancing the burning velocity of NH_3/C_2H_4/Air mixtures.

Ignition delay time (IDT) is a crucial parameter for assessing burner ignition and flame-holding stability, as well as a key metric for validating chemical reaction mechanisms[20]. Species profiles (SP) reflect the dynamic evolution of key components, radicals, pollutants, etc., during combustion processes, providing insights into critical chemical reaction mechanisms of fuels. The IDT of NH_3/O_2/Ar mixtures was determined by Mathieu et al.[21] using a shock tube. Their results demonstrated that lean mixtures exhibited relatively short IDT at elevated pressures, whereas the equivalence ratio showed minimal effect under low-pressure conditions. Furthermore, increased pressure was observed to enhance ignition promotion. Shu et al.[22] further expanded the experimental conditions of Mathieu and obtained similar conclusions. However, they pointed out that under lean fuel conditions with a pressure exceeding 20 bar, the IDT was longer. He et al.[23] measured the IDT of NH_3/O_2 and $NH_3/H_2/O_2$ mixtures using a rapid compression machine (RCM). Their results demonstrated that the addition of H_2 increased the fuel reactivity and promoted ignition, while the equivalence ratio varied depending on the amount of hydrogen added. Dai et al.[24] and Chen et al.[25] also investigated the IDT of $NH_3/H_2/O_2$ mixtures and observed a consistent trend with the work of He et al.[23]. However, Dai et al. pointed out that under any pressure, the ignition of NH_3 would slow down with the increase in the equivalence ratio. Peng et al.[26] explored the influence of the fuel concentration on ignition. The increase in the fuel concentration would intensify the reactions of NH_3 with more important radicals, thus promoting ignition. Regarding the species concentration, Dagaut et al.[27] investigated the oxidation of NH_3 under different NO concentrations using a jet-stirred reactor (JSR) and explained the interaction between NH_3 and NO. Manna et al.[28] conducted an in-depth study on the oxidation and pyrolysis of ammonia. They found that during the ammonia reaction process, the concentrations of NO and H_2 increased monotonically, while H_2 first increased, then decreased, and finally reached a maximum value. During the pyrolysis process, H_2 increased monotonically, and the yield under Ar-H_2O dilution was lower than that under Ar-only dilution. Osipova et al.[29] experimentally investigated the oxidation of ammonia and ammonia/hydrogen mixtures. Their results demonstrated that hydrogen addition promoted the formation of H, O, and OH radicals, enabling their generation at significantly reduced temperatures. However, Sabia et al.[30] explored the combustion of ammonia under N_2 dilution and found that NO had the highest concentration under lean fuel conditions, while H_2 had the highest concentration under rich fuel conditions.

Recent years have witnessed significant advancements in ammonia research as a zero-carbon fuel, with mechanisms underlying its combustion process developing rapidly, as indicated in Table 1. Since 2015, a variety of typical ammonia or ammonia-blended combustion mechanisms have been developed. However, it is worth noting that most of these mechanisms are designed for binary or multi-component fuels blended with ammonia, and their validation scopes are relatively narrow, usually limited to certain specific combustion characteristics and carried out under limited operating conditions. For example, based on Song's model[31], Otomo et al.[32] optimized the kinetic parameters of reactions related to NH_2, HNO, N_2H_2, etc., and constructed a combustion mechanism for NH_3/H_2/Air, and only verified it for LBV. Similarly, based on Mei's model[9], Zhang et al.[33] updated the thermodynamic parameters of key species such as NH_2, NH, and NNH, and proposed a kinetic mechanism for predicting the combustion behavior of NH_3 and NH_3/H_2

Table 1. Typical combustion mechanism of ammonia and ammonia-blended fuels.

Author	Year	Number of species/reactions	Fuel/oxidizer	Properties	Ref.
Mathieu et al.	2015	54/278	NH_3/O_2/Ar	IDT	[21]
Song et al.	2016	32/204	$NH_3/O_2/N_2$	SP	[31]
Otomo et al.	2018	32/213	NH_3/H_2/Air	LBV/IDT	[32]
Mei et al.	2019	38/265	$NH_3/O_2/N_2$	LBV/IDT	[9]
Han et al.	2020	35/174	NH_3/H_2/Syngas/Air	LBV/IDT	[2]
Zhang et al.	2021	38/263	NH_3/H_2/Air	SP	[33]
Bertolino et al.	2021	38/264	NH_3/Air	LBV/IDT/SP	[35]
Shrestha et al.	2021	125/1,099	NH_3/H_2/Air	LBV	[13]
Dagaut et al.	2022	47/257	NH_3/NO/Air	SP	[27]
Zhou et al.	2023	169/1,268	NH_3/H_2 /CO/CH_4/Air	LBV	[17]
Wang et al.	2023	35/178	$NH_3/H_2/O_2$/Air	LBV	[36]
Zhu et al.	2024	43/312	NH_3/Air; NH_3/H_2/Air	LBV/IDT/SP	[37]
Shrestha et al.	2025	285/2,364/38/307	NH_3/Methanol/Ethanol/Air/NH_3/H_2/CO/Air	LBV/IDT	[34]

blends. However, their validation also mainly focused on the changes in components. Shrestha et al.[34] conducted a comprehensive investigation into the oxidation kinetics of ammonia (NH_3) blended with methanol (CH_3OH) and ethanol (C_2H_5OH) under various conditions. They measured laminar flame speeds and ignition delay times of NH_3–alcohol mixtures, and developed a detailed kinetic model capable of accurately predicting the combustion characteristics of both pure NH_3 and NH_3-based fuel blends. Therefore, the development of an ammonia kinetic mechanism that can cover a wider range of operating conditions and meet multi-target requirements urgently needs to be studied.

As a powerful molecular simulation technique, Reactive force field molecular dynamics (ReaxFF MD) provides the capability to capture the precise reaction state at any given time point and track the detailed temporal evolution of all chemical species during combustion. This method has been widely applied to the study of fuel thermochemical reactions, such as pyrolysis[38] and combustion[39–42], to deeply explore product distribution and reaction mechanisms during fuel reactions. So as to deeply explore the product distribution and reaction channels during the fuel combustion process. Globally, the ReaxFF MD method has been employed by scholars to study the reaction mechanisms underlying ammonia and its blend combustion.

For example, Zhang et al.[38] employed ReaxFF MD simulations to study coal-ammonia co-pyrolysis at temperatures between 3,000 and 3,500 K. Their results revealed that the presence of coal markedly reduced the activation energy required for ammonia pyrolysis, thereby accelerating its decomposition. Huang et al.[39] utilized ReaxFF MD to examine the effect of H_2 on NH_3 combustion at different temperatures, systematically analyzing the pathway from NH_3 to NO. They found that adding hydrogen increased the production of H and OH radicals during ammonia combustion, thereby enhancing the combustion rate, with nitrogen-containing intermediates like HNO primarily reacting with OH and HO_2 to form NO_x. Zhang et al.[40] explored the combustion behavior under fuel-lean to fuel-rich conditions at temperatures of 2,400–3,200 K with varying NH_3/CH_4 blending ratios, showing that there was no competitive relationship between ammonia and methane combustion; instead, methane addition enhanced ammonia reactivity and accelerated NH_3 consumption. Guo et al.[42] investigated the combustion behavior and product distribution of NH_3/CH_4 at different temperatures and oxygen contents, revealing the micro-mechanism of NH_3/CH_4 combustion. Wang et al.[43] studied the combustion process of NH_3/CH_4 in air under high temperature and pressure, finding that these conditions accelerated NH_3 consumption and influenced NO_x production. Hong et al.[41,44] simulated the co-combustion behavior of coal and ammonia and NO formation characteristics under different oxygen equivalence ratios in the range of 2,500–3,500 K, discovering a competitive relationship between ammonia and coal, with ammonia dominating oxygen competition, resulting in an accelerated ammonia oxidation rate at the expense of coal oxidation, influenced mainly by temperature, blending ratio, and oxygen concentration. Wang et al.[45] examined the impact of different ionization degrees on NH_3 combustion reaction rates and NO_x formation, analyzing the mechanism of NO_x formation. They found that at 2,000 K, NO concentration was lowest when the ionization ratio was 25%, reaching a maximum when the ionization ratio increased to 50%.

In conclusion, ammonia is widely recognized as a promising zero-carbon fuel with substantial potential to enable the decarbonization of energy systems. However, its combustion mechanisms remain incompletely characterized, with critical parameters, including pollutant formation pathways, lacking comprehensive data. The ReaxFF MD method has emerged as a critical computational framework for investigating ammonia combustion processes and reaction mechanisms. However, mechanistic research on ammonia fuel remains nascent, with limited exploration of ReaxFF MD-based combustion analysis. This study implements ReaxFF MD simulations to examine ammonia combustion under varying equivalence ratios and temperatures. By tracking the temporal evolution of key radicals and products, we elucidate ammonia's primary reaction networks and molecular-level formation pathways. Furthermore, novel reaction pathways identified through ReaxFF MD are integrated with established mechanisms to construct a comprehensive ammonia combustion framework, validated across multiple combustion characteristics.

Simulation methods

ReaxFF MD method

The reactive force field was developed by the Vain group[46]. This force field is grounded in the concept of bond order (BO), which quantifies the formation and rupture of chemical bonds, thereby enabling the simulation of interactions within chemical systems. Bond order is fundamentally dependent on interatomic distances and can be computed directly from them. Atomic interactions are governed by bond order, and by monitoring the evolution of bond orders throughout simulations, the formation and dissociation of chemical bonds can be accurately determined. This method provides a dynamic description of atomic and molecular interactions without relying on predefined reaction sites, as required by classical potentials[46]. Additionally, it allows for the efficient calculation of larger molecular systems with relatively low computational resources. The reactive force field incorporates the system's total energy equation and the empirical bond order formula, as described in[47]:

$$E_{system} = E_{bond} + E_{over} + E_{under} + E_{lp} + E_{angle} + E_{torsion} + E_{vdWaals} + E_{Coulomb} \tag{1.1}$$

$$\begin{aligned} BO_{ij} &= BO_{ij}^{\sigma} + BO_{ij}^{\pi} + BO_{ij}^{\pi\pi} \\ &= \exp\left[p_{bo1}\left(\frac{r_{ij}}{r_o^{\sigma}}\right)^{p_{bo2}}\right] + \exp\left[p_{bo3}\left(\frac{r_{ij}}{r_o^{\pi}}\right)^{p_{bo4}}\right] + \exp\left[p_{bo5}\left(\frac{r_{ij}}{r_o^{\pi\pi}}\right)^{p_{bo6}}\right] \end{aligned} \tag{1.2}$$

The above equation represents the system's total energy E_{system}, where E_{bond}, E_{over}, E_{under}, E_{lp}, E_{angle}, $E_{torsion}$, $E_{vdWaals}$ and $E_{Coulomb}$ are the bond energy, over-coordination energy, under-coordination energy, lone pair energy, angle energy, torsion potential energy, van der Waals interaction energy, and Coulomb interaction energy, respectively. BO_{ij} represents the bond order between atoms i and j, primarily composed of three components: sigma σ bonds, π bonds, and $\pi\pi$ bonds. Here, r_{ij}, r_o, and p_{bo} denote the interatomic distance, equilibrium bond length, and empirical parameters, respectively.

Due to its broad application in molecular dynamics simulations, ReaxFF is capable of modeling chemical reactions and thermodynamic properties at the microscopic scale. It has been applied in fields such as high-temperature pyrolysis[38], combustion[39–42].

In this study, the ReaxFF submodule within the open-source LAMMPS program[48] was employed to simulate and analyze the ammonia combustion process. Post-simulation analysis was carried out using the Ovito software[49] and the RMD_Digging program developed by Liu et al.[50], with a particular focus on the evolution of key product distributions and the reaction pathways of ammonia combustion.

This study provides a comprehensive investigation into the effects of oxygen concentration and temperature on the ammonia combustion process over a wide range of conditions, encompassing equivalence ratios from 0.5 to 1.5 (covering both fuel-lean and fuel-rich regimes) and temperatures between 2,800 and 3,600 K. The stoichiometric combustion of ammonia is described by the following reaction:

$$4NH_3 + 3O_2 = 2N_2 + 6H_2O \quad (1.3)$$

Three distinct ammonia/oxygen simulation boxes were constructed, each containing 80 ammonia molecules along with 120, 60, and 40 oxygen molecules, respectively. These boxes were configured with periodic boundary conditions (i.e., ppp boundary conditions in LAMMPS). The simulation systems outlined in Table 2 were designed by varying the temperature. Figure 1 provides a visualization of the ammonia/hydrogen simulation system with an equivalence ratio of 1.0.

The simulations employed the C/H/N/O ReaxFF force field originally parameterized by Zhang et al.[51] for N_2H_4 decomposition studies. This framework was subsequently adapted by Hong et al.[44] and Wang et al.[45] for NH_3/CH_4 combustion simulations, demonstrating predictive accuracy for NH_3 combustion characteristics. System initialization involved conjugate gradient energy minimization to eliminate molecular overlap artifacts. NVT ensemble simulations with 0.1 fs timestep over 500 ps duration were conducted across 2,800–3,600 K for varying equivalence ratios. Atomic trajectories sampled at 1 ps intervals enabled combustion process tracking.

Post-processing utilized RMD_Digging's species_analysis and chemi_mechanism modules to extract bond-order evolution, product formation patterns, and reactive trajectories. Ovito visualization software mapped reactant-product correlations, enabling mechanistic pathway reconstruction.

Table 2. Information about each simulation system.

System	Temperature (*K*)	Equivalent ratio	Number of molecules		Size (nm)
			NH_3	O_2	
1	3,000	0.5	80	120	22.1029 × 22.1029 × 22.1029
2	3,000	1.0	80	60	18.9575 × 18.9575 × 18.9575
3	3,000	1.5	80	40	17.6354 × 17.6354 × 17.6354
4	2,800	1.0	80	60	18.9575 × 18.9575 × 18.9575
5	3,200	1.0	80	60	18.9575 × 18.9575 × 18.9575
6	3,400	1.0	80	60	18.9575 × 18.9575 × 18.9575
7	3,600	1.0	80	60	18.9575 × 18.9575 × 18.9575

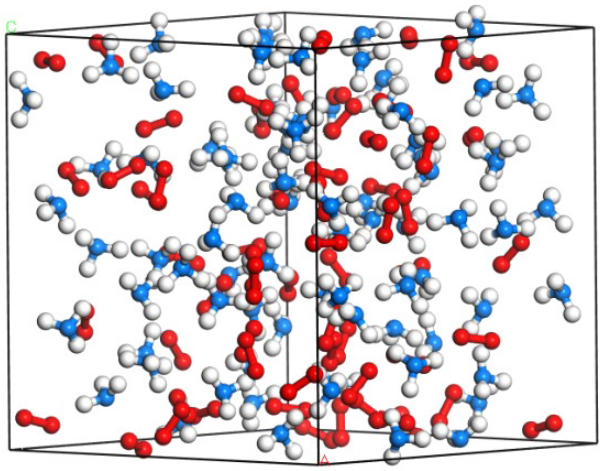

Fig. 1 Ammonia/oxygen premixed system (Equivalence ratio = 1.0, N is blue, H is white, O is red).

Mechanism construction, optimization, and validation method

Recent advances have yielded various ammonia-based combustion mechanisms, predominantly developed for multi-fuel blends and validated under limited operating conditions. This study establishes a predictive kinetic framework through hierarchical integration of NH_3 combustion models with ReaxFF MD simulations. The mechanism demonstrates multi-target validation across laminar burning velocities, ignition delay times, and species profiles under extended conditions: temperatures (298–1,900 K), pressures (1–40 atm), and equivalence ratios (0.5–2.0). Critical reaction parameters are re-evaluated through sensitivity analysis to optimize model fidelity.

Combustion simulations were implemented via Cantera's Python interface[52] using three numerical approaches: (1) Adiabatic freely propagating flames for LBV determination in NH_3/Air systems; (2) Constant-volume reactors for IDT prediction; (3) Perfectly stirred reactors for species evolution analysis. Parameter configurations strictly followed experimental protocols, with model validation conducted against benchmark datasets and comparative mechanism assessments.

ReaxFF MD results and discussion

This study focuses on ammonia combustion, specifically examining how varying equivalence ratios and temperatures influence the combustion process. The reaction pathways involved in ammonia combustion were also analyzed. Systems 1, 2, and 3 are employed to explore the influence of equivalence ratios, while systems 2, 4, 5, 6, and 7 are utilized to assess the effect of temperature on the combustion dynamics. To gain deeper insight into the reaction mechanism of ammonia, this study investigated the pyrolysis process at 3,000 K using ReaxFF MD simulations, as illustrated in Supplementary File 1 (Fig. S1). The results indicate that NH_3 initially undergoes dehydrogenation to form NH_2 and H radicals. The generated H radicals further react with NH_3 to produce NH_2 and H_2. The NH_2 radicals are rapidly consumed through reaction channels such as $NH_2 = NH + H$ and $NH_2 + H = NH + H_2$, yielding NH and H_2. Due to their high reactivity, NH and N radicals participate in reactions such as $NH + H = N + H_2$ and $H + H = H_2$, maintaining the radical concentrations at relatively low levels. This process also promotes a continuous increase in H_2 formation. Furthermore, as NH_2 dehydrogenates to form NH, these intermediate species (NH_2 and NH) proceed through a series of direct and indirect pathways toward N_2 formation, including reactions such as $NH_2 + N = N_2 + H_2$, $NH = N + H$, $NH + H = N + H_2$, $NH + NH = N_2 + H_2$, and $N + N = N_2$. These reactions are also accompanied by H_2 production, ultimately resulting in faster accumulation and a larger yield of H_2 compared to N_2 during ammonia pyrolysis. Additionally, minor reaction channels such as $NH_2 + NH_2 = N_2H_4$, $N_2H_4 + NH = N_2H_3 + NH_2$, and $N_2H_4 = N_2H_2 + H_2$ are also observed in the process. The reaction mechanisms of ammonia pyrolysis described above must also be given priority consideration when developing combustion mechanisms for ammonia.

Influence of equivalence ratio on ammonia combustion

Figure 2 depicts key combustion metrics at 3,000 K for equivalence ratios (ϕ = 0.5, 1.0, 1.5). Lean conditions (ϕ = 0.5) exhibit near-total NH_3 consumption with O_2 surplus, whereas stoichiometric combustion (ϕ =1.0) achieves complete reactant depletion. Fuel-rich systems (ϕ = 1.5) retain unreacted NH_3. These consumption patterns align quantitatively with literature benchmarks[40], validating the C/H/N/O ReaxFF force field's fidelity in ammonia combustion dynamics. While equivalence ratio variations minimally alter the primary reaction sequence, residual reactants engage in secondary pyrolysis upon partner depletion – O_2 in lean or NH_3 in rich environments.

Figure 3 depicts the changes in key radicals and products over time during ammonia combustion at different equivalence ratios when the temperature is 3,000 K. Figure 3a shows the variation curve of NH_2 radical over time. Under fuel-rich conditions, the peak concentration of NH_2 radicals is moderately lower than that observed under fuel-lean to stoichiometric conditions, with a small residual amount of NH_2 remaining. This behavior can be attributed to the excess ammonia present under fuel-rich conditions, which moderates the formation of NH_2 radicals, leading to a reduced peak value. However, the excess NH_3 undergoes thermal decomposition, leading to an increase in NH_2 through reactions such as R1:

$$NH_3(+M) = NH_2 + H(+M) \quad (R1)$$

Figure 3b and c present the temporal evolution of OH and H_2 concentrations, respectively. As shown in Fig. 3b, the peak concentration of OH radicals is highest under fuel-lean conditions and lowest under fuel-rich conditions. In Fig. 3c, a larger amount of H_2 persists under fuel-rich conditions. Under both fuel-lean and stoichiometric conditions, H_2 is gradually consumed after reaching its peak. The peak H_2 concentration under stoichiometric conditions is higher than that under fuel-lean conditions, and the consumption process occurs over a longer duration. These findings align with both the OH/H_2 variation trends observed in lean combustion conditions[44] and the H_2 behavioral characteristics documented under fuel-rich environments[41]. The observed kinetic behavior likely originates from radical oversaturation mechanisms inherent to fuel-lean combustion regimes, where molecular oxygen (O_2) serves dual roles as both oxidizer and chain-branching promoter, thereby accelerating radical pool proliferation through enhanced H-abstraction efficiency. After the ammonia fuel is completely reacted, there are still surplus oxygen molecules and O radical participating in the reaction process, through reaction channels such as R2–R4:

$$H + O_2 = O + OH \quad (R2)$$

$$H + O = OH \quad (R3)$$

$$O + H_2 = OH + H \quad (R4)$$

This results in the generation of more OH radical and accelerates the consumption of H_2, leading to a higher amount of OH but a lower production and rapid consumption of H_2 under lean-fuel conditions. Under rich-fuel conditions, due to the insufficient oxygen content itself, the complete reaction of NH_3 is restricted, resulting in the least amount of OH generated. The remaining H_2 may be because after the existing oxygen consumes part of the ammonia, there is still an excess of ammonia, causing some of the ammonia to decompose and participate in the reaction process. H_2 is a key intermediate species during ammonia combustion. Its formation primarily relies on pathways R5 and R6, both of which originate from H radicals. Therefore, the consumption channels of H radicals directly influence H_2 generation. Under conditions with sufficient oxygen, such as when the equivalence ratio is greater than or equal to 1, H radicals tend to react with O_2 to form species like OH, which suppresses pathways such as NH_3 + H = NH_2 + H_2 and H + H = H_2. Additionally, the resulting OH can further consume NH_3. As a result, H_2 does not accumulate effectively in oxygen-rich environments. In contrast, at an equivalence ratio of 1.5, H_2 can accumulate over an extended period before being consumed later. This behavior is consistent with the results shown in Fig. 3c. This leads to an excess of H radical under rich-fuel conditions, through a series of reactions such as R5 and R6:

$$NH_3 + H = NH_2 + H_2 \quad (R5)$$

$$H + H = H_2 \quad (R6)$$

result in additional H_2 formation under fuel-rich conditions.

Figure 3d shows the curve of NO changing with time. As expected, the emission of NO is mainly concentrated under lean-fuel to stoichiometric ratio conditions. This may be because subsequent reactions promote the further conversion of NO to N_2, resulting in a decrease in NO. NO formation becomes negligible under fuel-rich conditions due to oxygen-deficient combustion environments. This is probably due to the insufficient oxygen atmosphere, which restricts the formation of NO, leading to the emission of more

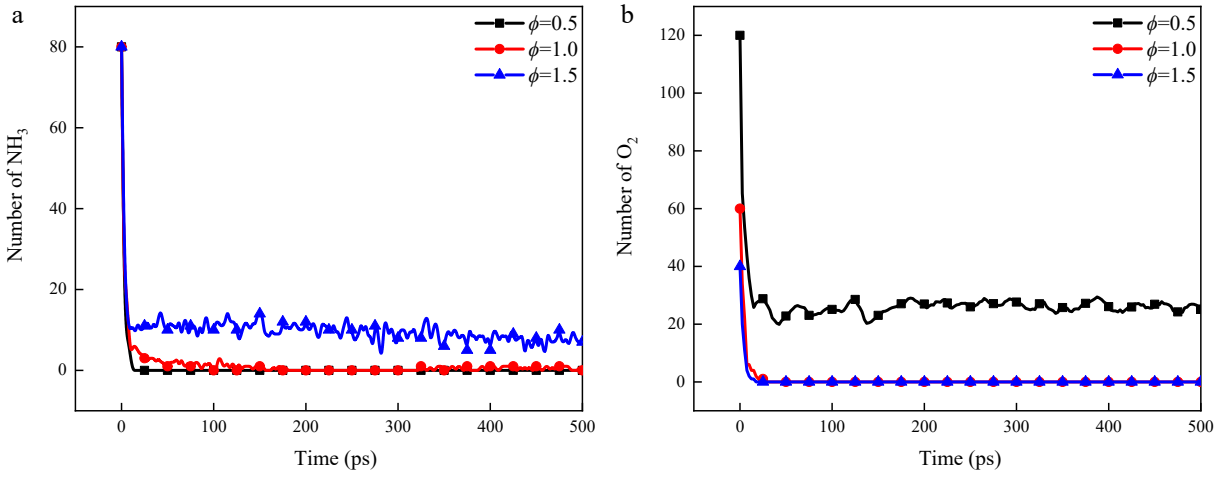

Fig. 2 Evolution of main reactants at different equivalent ratios.

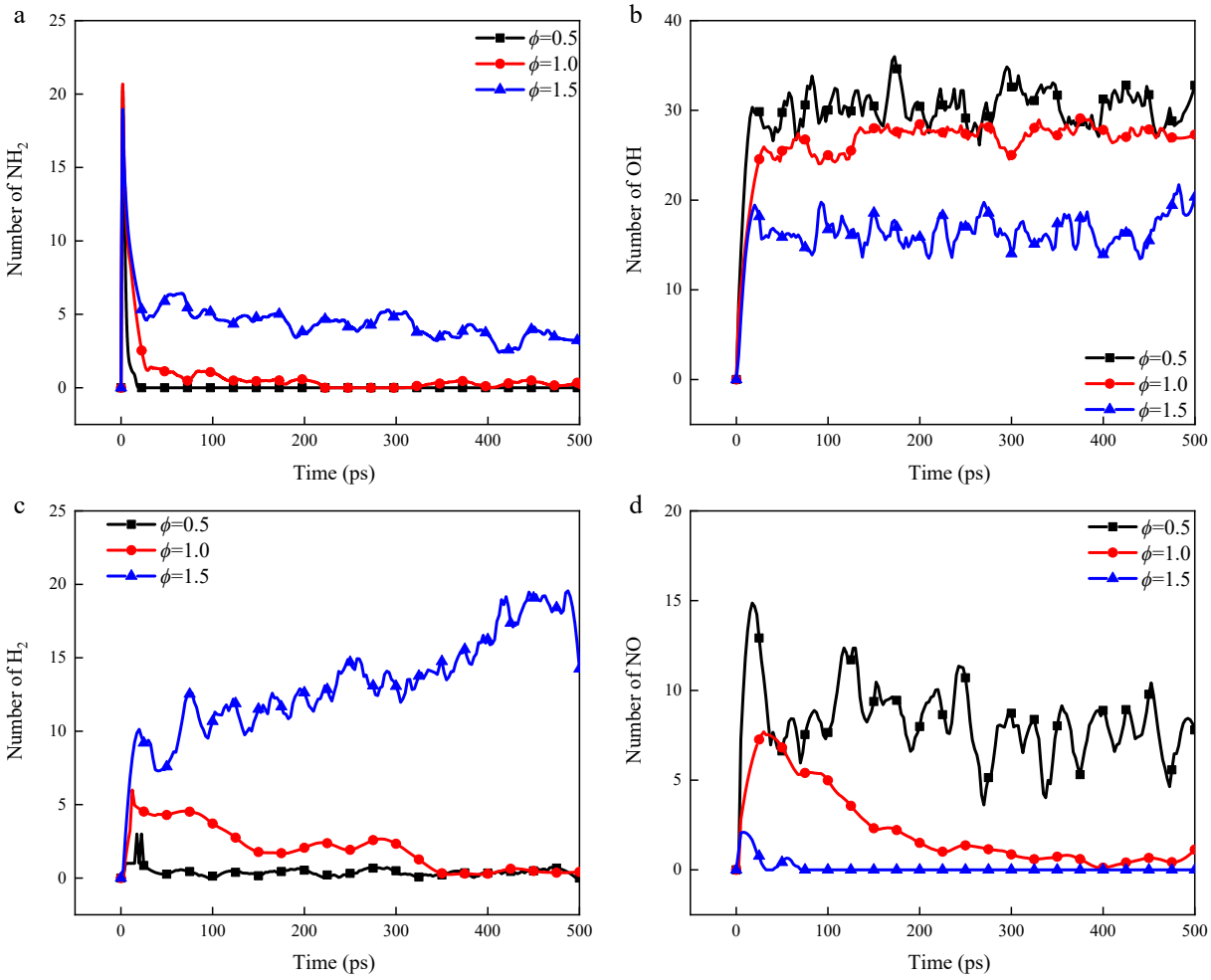

Fig. 3 Temporal evolution of main radicals and products at different equivalence ratios.

unreacted ammonia. Variations of H, O_2, and N_2 under different equivalence ratios are presented in Supplementary File 1 (Fig. S2).

Influence of temperature on ammonia combustion

Figure 4 tracks the kinetic progression of NH_3/O_2 consumption at ϕ = 1.0 across thermal gradients. Thermal acceleration markedly enhances decomposition kinetics, with elevated temperatures (> 3,000 K) inducing earlier combustion initiation compared to reference studies[41,44], a manifestation of our extended thermal regime investigation.

Distinct differential depletion kinetics emerge: Oxygen achieves complete conversion within 50 ps at 2,800 K, while residual NH_3 persists at 21% concentration until 125 ps. This reactant hierarchy (O_2 > NH_3) validates the force field's predictive capacity for sequential consumption patterns in ammonia oxidation.

Figure 5 delineates temperature-dependent radical dynamics and product evolution at ϕ = 1.0 (see Supplementary File 1, Fig. S3 for full speciation). NH_2 radicals exhibit rapid peaking followed by accelerated depletion at elevated temperatures (Panel A). Temperature-dependent peak amplification manifests in OH/H_2 profiles (Panels B–C), with OH displaying thermal stabilization (sustained concentration post-peak) contrasting H_2's transient intermediate behavior. NO formation kinetics (Panel D) confirm literature-consistent[44] thermal acceleration effects, though divergent post-peak trajectories emerge under our equivalence ratio constraints.

Reaction mechanism and pathway analysis

Figure 6 explores the ammonia combustion reaction network at an equivalence ratio of 1.0 and a temperature of 3,000 K. Figure 6a illustrates the nitrogen atom transfer pathways during the ammonia combustion process, while Fig. 6b depicts the hydrogen atom transfer pathways. The red lines represent the newly discovered paths.

In Fig. 6a, it is shown that ammonia initially undergoes hydrogen abstraction reactions, predominantly producing NH_2 radicals. These NH_2 radicals further convert into NH radicals, with only a small fraction of NH_3 directly forming NH radicals. The subsequent reaction pathways of NH_2 radicals are diverse. They can be directly or indirectly converted to N_2 through the generation of radicals such as N_2H_4, N_2H_3, and N_2H_2, or they can be converted to NO through the generation of NH_2OH, HNOH, and HNO, which is similar to that in previous studies[36,45]. Notably, this study identifies a small amount of NH_2OH, which primarily contributes to the indirect formation of HNOH and H_2NO through reactions R7–R10:

$$NH_2 + OH = NH_2OH \quad (R7)$$

$$NH_2OH = NH + H_2O \quad (R8)$$

$$NH_2OH + H = H_2NO + H_2 \quad (R9)$$

$$NH_2OH + OH = H_2NO + H_2O \quad (R10)$$

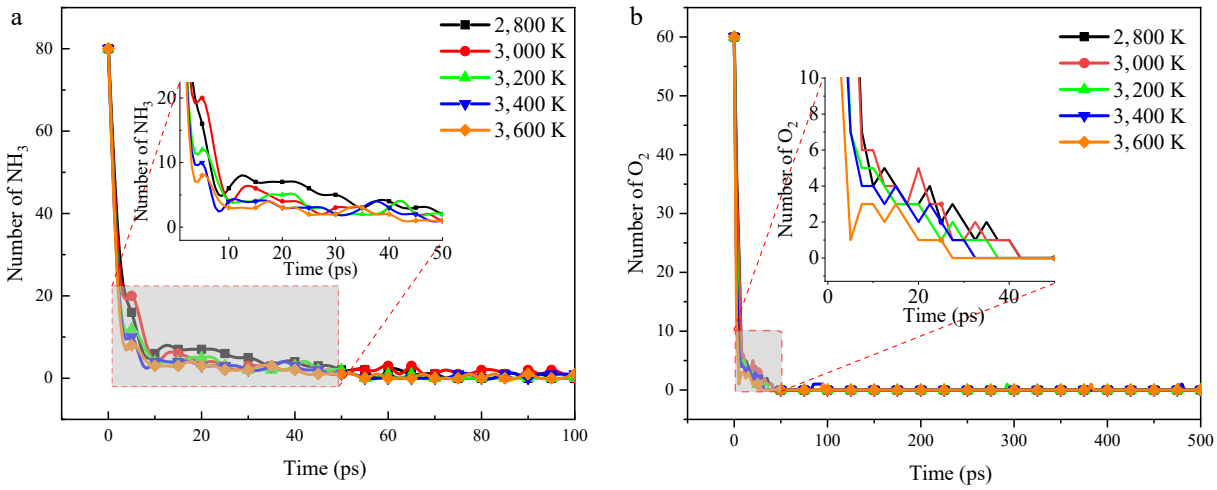

Fig. 4 Variation curves of NH_3 and O_2 with time at different temperatures.

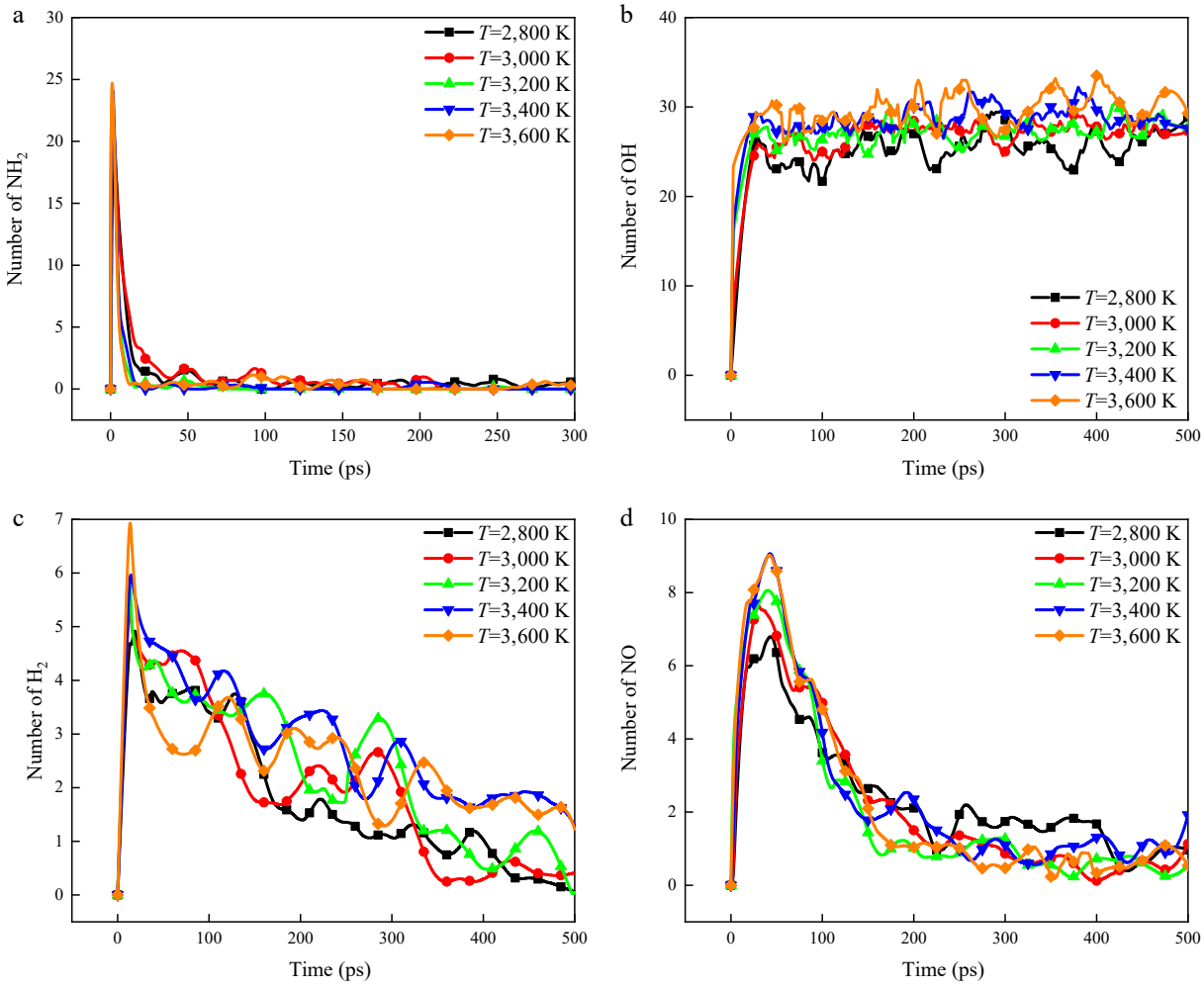

Fig. 5 Variation curves of radicals and formation products with time at different temperatures.

Regarding the reaction pathways for the formation of N_2, they can be summarized into two relatively major paths. One approach is the conversion to form NNH. NH can directly form NNH through reaction R11:

$$NH + NO = NNH + O \quad (R11)$$

Alternatively, NH can react with N_2H_4, leading to a sequence of reactions: NH → (N_2H_4 → N_2H_3) → N_2H_2 → NNH. In the analysis of N_2H_2, it was found that, in addition to being formed by NH_2, NH, and N_2H_3, a very small amount of N_2H_3OH can also generate N_2H_2 through reaction R12:

$$N_2H_3OH = N_2H_2 + H_2O \quad (R12)$$

This intermediate has not been mentioned in other literature. It is noteworthy that NNH and N_2 can interconvert through reactions, although initially, NNH predominantly converts to N_2. As N_2 accumulates, it gradually begins to convert back into NNH.

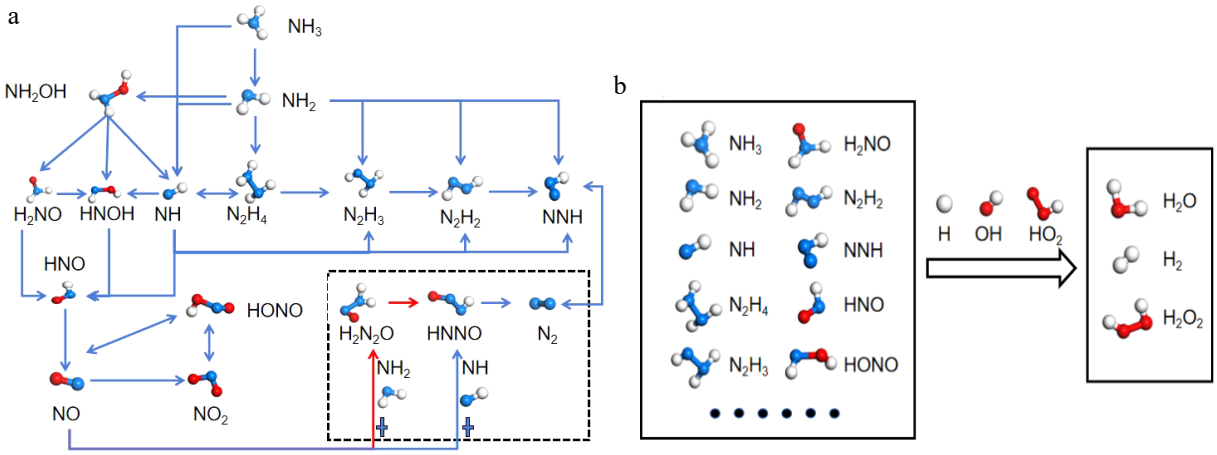

Fig. 6 Reaction path of ammonia combustion.

The other major pathway is the formation of NO. It can be converted to form NO through the route of $NH_2 \rightarrow NH (\rightarrow HNOH) \rightarrow HNO \rightarrow NO$ (that is, the route in the blue dashed box), which is consistent with the description[36,45]. What is relatively different is that during this process, it is found that H_2NO, as an isomer of HNOH, can also generate HNO, but the contribution of H_2NO is relatively large. NO can be produced through the reactions of HNO and HONO radicals, with HNO being the primary contributor. HONO formation is closely related to NO and NO_2 and can be converted through reactions R13–R17:

$$NO + OH = HONO \quad (R13)$$

$$NO + HO_2 = NO_2 + OH \quad (R14)$$

$$HONO + H = NO + H_2O \quad (R15)$$

$$HONO + OH = NO_2 + H_2O \quad (R16)$$

$$H_2NO + NO_2 = HNO + HONO \quad (R17)$$

The conversion relationships among HONO, NO, and NO_2 align with those described in the literature[45], although in literature[37], HONO is not considered a primary interconversion species with NO but is only mentioned in the mechanism files. Notably, when the NO production significantly increases, it can lead to the formation of two intermediate species, H_2N_2O and HNNO, through reactions R18–R20:

$$NO + NH_2 = H_2N_2O \quad (R18)$$

$$NO + NH = HNNO \quad (R19)$$

$$H_2N_2O = HNNO + H \quad (R20)$$

Prior to this, these intermediates were only mentioned in the literature[45], but with some distinctions. The analysis in the study by Wang et al.[45] pertains to fuel-lean conditions, and H_2N_2O was not mentioned in the absence of ionization, being identified only under conditions with a high degree of ionization. It can convert to N_2 through reactions R21–R23:

$$NH_2 + NO = H_2N_2O \quad (R21)$$

$$H_2N_2O + H = HNNO + H_2 \quad (R22)$$

$$HNNO = N_2 + OH \quad (R23)$$

with NO being relatively less prevalent under ionized conditions. However, in this study, H_2N_2O and HNNO are both detected under stoichiometric conditions, where NO is observed to decline after reaching a certain concentration due to the presence of H_2N_2O and HN_2O, leading to an increase in N_2.

Figure 6b lists some species that contribute to the formation of H_2, H_2O, and H_2O_2. The hydrogen atom transfer pathways in these nitrogen-hydrogen compounds tend to favor hydrogen abstraction reactions, which primarily promote the formation of H_2, H_2O, and H_2O_2. The generated H_2 mainly originates from the reactions of NH_3, NH_2, NH, and N_2H_4 with single hydrogen atoms, while H_2O is largely produced from the reactions between nitrogen-hydrogen compounds and OH radicals. Additionally, H_2O_2 formation mainly depends on reactions involving HO_2 radicals. Of course, aside from these pathways, other reactions with O atoms and other species or self-decomposition reactions can also produce H_2, H_2O, and H_2O_2, although their contributions are relatively minor.

Model construction and verification analysis

In this study, based on six well-performing NH_3 kinetic models, combined with the new reaction pathways obtained from ReaxFF MD, a relatively complete comprehensive kinetic mechanism model for NH_3 combustion is constructed by coupling. Moreover, the kinetic parameters of key reactions exerting a strong influence on combustion characteristics are updated and optimized. To validate the reliability and accuracy of the model, extensive comparisons are performed against existing experimental data for a wide range of ammonia combustion properties, including laminar burning velocity, ignition delay time, and species concentration profiles. Furthermore, kinetic analyses—such as reaction path and sensitivity analyses—are employed to elucidate the underlying reaction pathways and key mechanistic features of ammonia combustion.

Model construction

Seven NH_3 kinetic models demonstrating validated predictive accuracy for NH_3/Air and NH_3/H_2/Air combustion systems were systematically evaluated: Otomo model[32], Mei model[9], Han model[2], Zhang model[33], Wang model[36], Zhu model[37], and Shrestha model[34]. These mechanisms are selected based on their demonstrated fidelity in reproducing LBVs and ITDs across equivalence ratios and pressures. Figure 7 shows the comparison of each mechanism. Although these mechanisms can predict the combustion characteristics of ammonia,

they exhibit significant differences in reaction pathways, as shown in Supplementary File 1 (Fig. S4 and Table S1). Through the comparative study, it was found that the Mei model and the Zhang model showed good performance in the prediction of LBV, while the Zhu model showed good performance in the prediction of IDT. The Zhang model[33] was based on the Mei model[9] and updated the thermodynamic parameters of NH_2 and NH. Therefore, in this study, based on the hierarchical construction method, taking the Zhang model[33] as the foundation, changes were made by combining the newly added species and the changed reaction parameters in the Zhu model[37], and the new reaction paths discovered in the reactive molecular dynamics simulation are added.

The kinetic reaction mechanism is constructed through a coupling approach and primarily consists of three core components. The first component comprises validated sub-mechanisms for H_2, H_2O_2, and OH radicals. The H_2 sub-mechanism and related components have been comprehensively validated against experimental hydrogen combustion data by the Glarborg research group[53].

The second component addresses two distinct pathways for nitrogen species formation: (1) $NH_3 \rightarrow N_2$ pathway: Utilizes reaction parameters from the Zhang model[33]. (2) $NH_3 \rightarrow$ NOx pathway: Incorporates critical intermediates (HNNO, t-ONNH, c-ONNH) exclusively identified in the Zhu model[37], which contribute to NO_x formation, as demonstrated both in literature[54] and by our ReaxFF MD simulations. These intermediates have been systematically integrated into the current mechanism.

The third component incorporates novel reaction pathways identified through ReaxFF MD simulations, notably the H_2N_2O species - a newly characterized NO precursor. This marks the first integration of H_2N_2O into ammonia combustion kinetics (Supplementary File 1, Table S2 for mechanistic details). Reaction parameters for R2-1/R2-2 originate from NIST-curated studies[55–57], while R2-3/R2-4 parameters were derived through analogy to Zhu's framework[37].

To enhance NH_3/Air mixture combustion predictability, 21 key reactions (Supplementary File 1, Table S3) are calibrated through synergistic integration of Zhang's[33] and Zhu's[37] frameworks. These modifications primarily target: (1) LBV-sensitive reactions (R3–1 to R3–9), (2) IDT-sensitive reactions (R3–10 to R3–18), (3) Product-forming reactions (R3–19 to R3–21) for $NH_3/H_2O/NO$ generation. The final mechanism encompasses 351 reactions and 41 species, with combustion characteristic sensitivities detailed in subsequent analysis.

Model validation

Laminar burning velocity

This model systematically examines LBV across extensive operating conditions, spanning equivalence ratios of 0.8–1.6, pressures of 1–5 atm, and temperatures of 298–500 K. The results are compared and validated against experimental data in the literature[8–19], as shown in Fig. 8. For validations under additional operating conditions, Fig. S5 in the Supplementary File 1 is referenced. Specifically, Fig. 8a–d investigates the influence of temperature, while Fig. 8d, e focuses on the impact of pressure.

Under different temperatures (i.e., Fig. 8a–d), the current model predicts that laminar burning velocity increases continuously with rising temperature, peaking near an equivalence ratio of 1.1, aligning with literature findings[10]. At 298 K and 1 atm, ammonia's low flame speed makes it susceptible to buoyancy effects, introducing minor deviations in experimental data under lean- and rich-fuel conditions. Nonetheless, the model's predictions broadly capture experimental trends from lean-fuel to peak equivalence ratios, with slight discrepancies only under moderately rich-fuel conditions. The Otomo model[32] exhibits comparable accuracy to the current model. Predictions from the Mei[9], Han[2], and Zhang[33] models moderately overestimate experimental values, whereas the Wang[36] and Zhu[37] models show significant deviations. At temperatures above 298 K, the current model demonstrates robust performance in predicting laminar burning velocity, covering 90% of experimental data with a minor underestimation at 500 K. The Otomo model[32] achieves good agreement at 473 K but underestimates result under other conditions. The Mei[9] and Zhang[33] models remain slightly over predictive, while the Wang[36] and Zhu[37] models perform worst, consistently overestimating experimental results. The Han model[2] underpredicts at 373 K but overestimates under all other conditions.

Under different pressures (i.e., Fig. 8d–f), the current model's predictions at 3 and 5 atm show exact agreement with experimental values, with only a minor underestimation at 1 atm. The Mei[9] and Zhang[33] models demonstrate good accuracy at 1 atm but systematically overpredict under elevated pressures. The Otomo model[32] achieves partial agreement under fuel-rich conditions at 3 atm, underpredicts at 1 atm, and overestimates at 5 atm. The Wang[36] and Zhu[37] models remain the least accurate across all conditions. The Shrestha model[34] generally overestimates the predictions of ammonia flame speed.

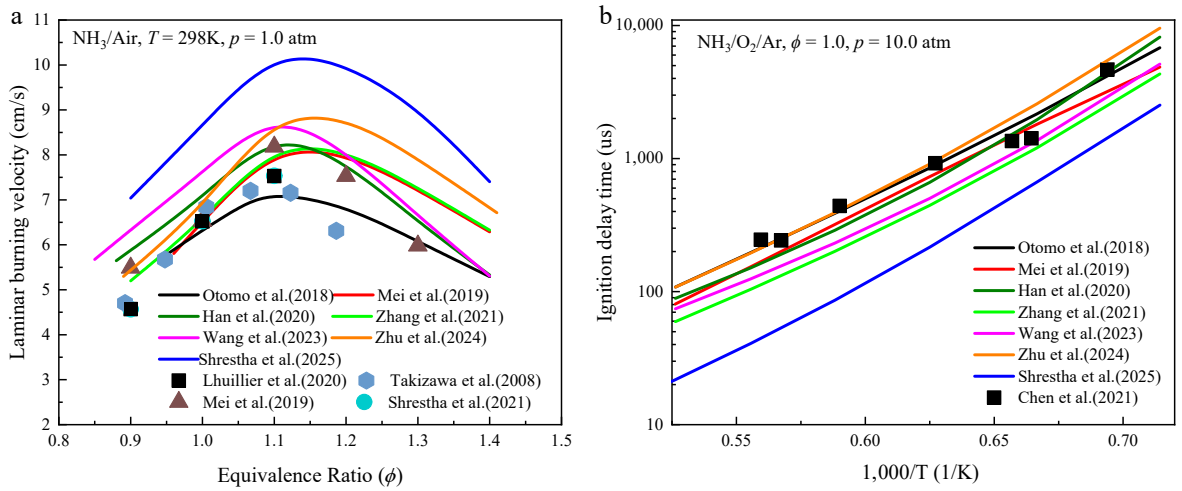

Fig. 7 Comparison of predictive capabilities of different mechanism. (The lines represent predictions seven comparative models, while the symbols correspond to experimentally measured data reported in Lhuillier et al.[10], Takizawa et al.[8], Mei et al.[9], Shrestha et al.[13], and Chen et al.[25]).

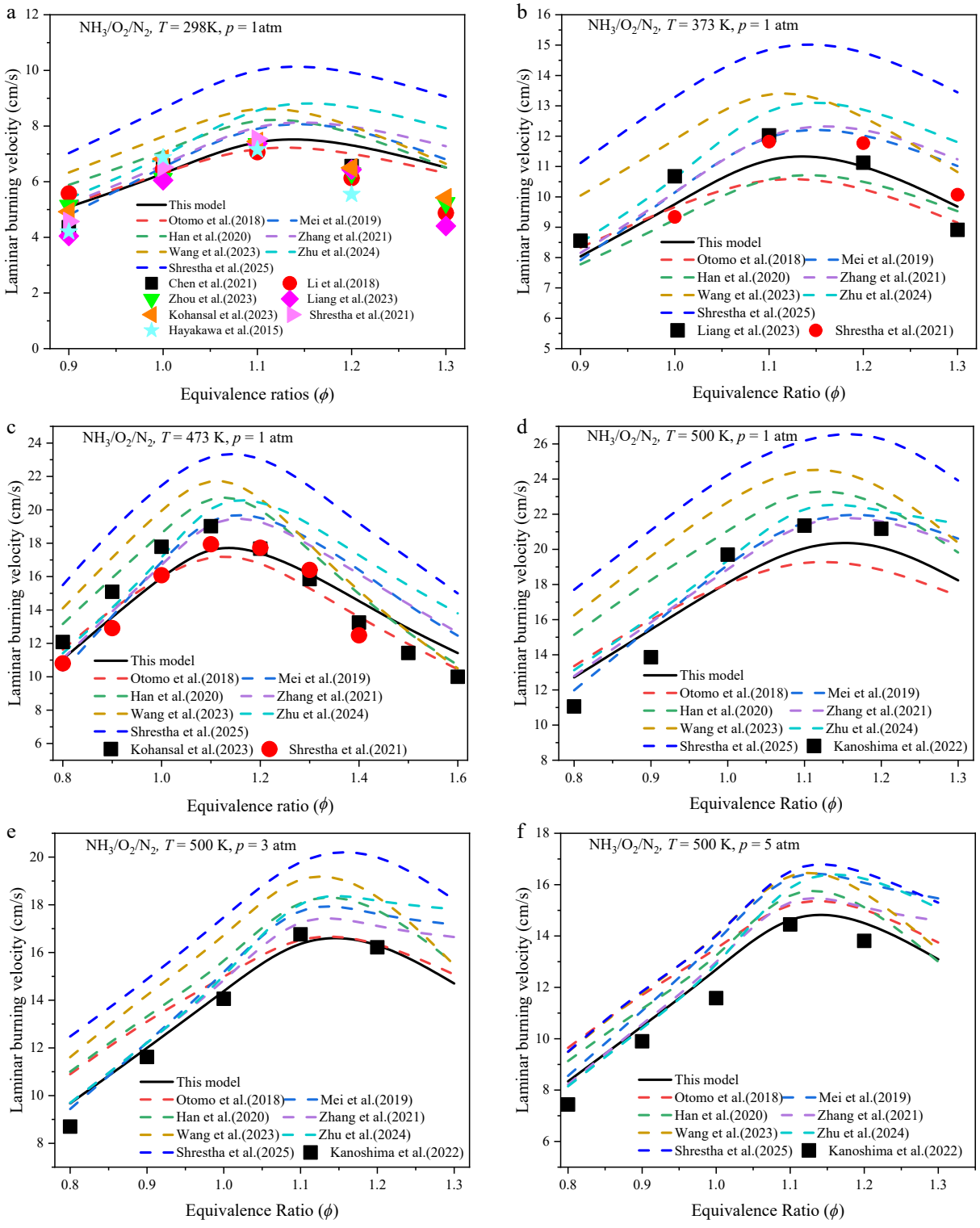

Fig. 8 Comparative verification of laminar burning velocity. (The line is the prediction result of this model and the other seven models, and the points are experimental data, from Hayakawa et al.[11], Chen et al.[12], Shrestha et al.[13], Kanshina et al.[14], Liang et al.[15], Zhou et al.[17], Kohansal et al.[18], and Li et al.[58]).

Ignition delay time

Validation is performed across a broad range of conditions, spanning lean-to-rich fuel (equivalence ratio 0.5–2.0), low-to-high pressure (1– 40 atm), and two dilution cases (Ar and N_2), as illustrated in Fig. 9. For additional validations, see Supplementary File 1 (Figs S6 and S7). Under Ar dilution, the current model exhibits excellent agreement with Chen's data, with only a slight overprediction at high temperatures under 10 atm. The Mei[9] and Zhu[37] models perform similarly to the current model. The Otomo model[32] underpredicts at low pressures, while the Han[2] and Wang[36] models generally overpredict. The Zhang model[33] shows the poorest accuracy. For N_2 dilution, the current model's predictions across

equivalence ratios of 0.5–2.0 align closely with experimental data. Notably, at an equivalence ratio of 1.0 and 20 bar pressure, the predictions exhibit an exact match with experimental values. Under these conditions, the Zhang model[33] improves significantly, mirroring the current model's trend. However, the Mei[9] and Zhu[37] models underpredict at low temperatures, and other models display limited accuracy. The Shrestha model[34] predicts ammonia ignition delay times relatively quickly at conditions of 10 atm and below, while its predictions are slower at conditions above 20 atm. In summary, the current model demonstrates robust predictive capability for ignition delay time across wide-ranging operating conditions.

Species profiles

Given that ammonia inherently contains nitrogen, its combustion can result in significant emissions of NO_x pollutants, which predominantly occur under fuel-lean to stoichiometric conditions. Consequently, research on ammonia combustion chemistry emphasizes

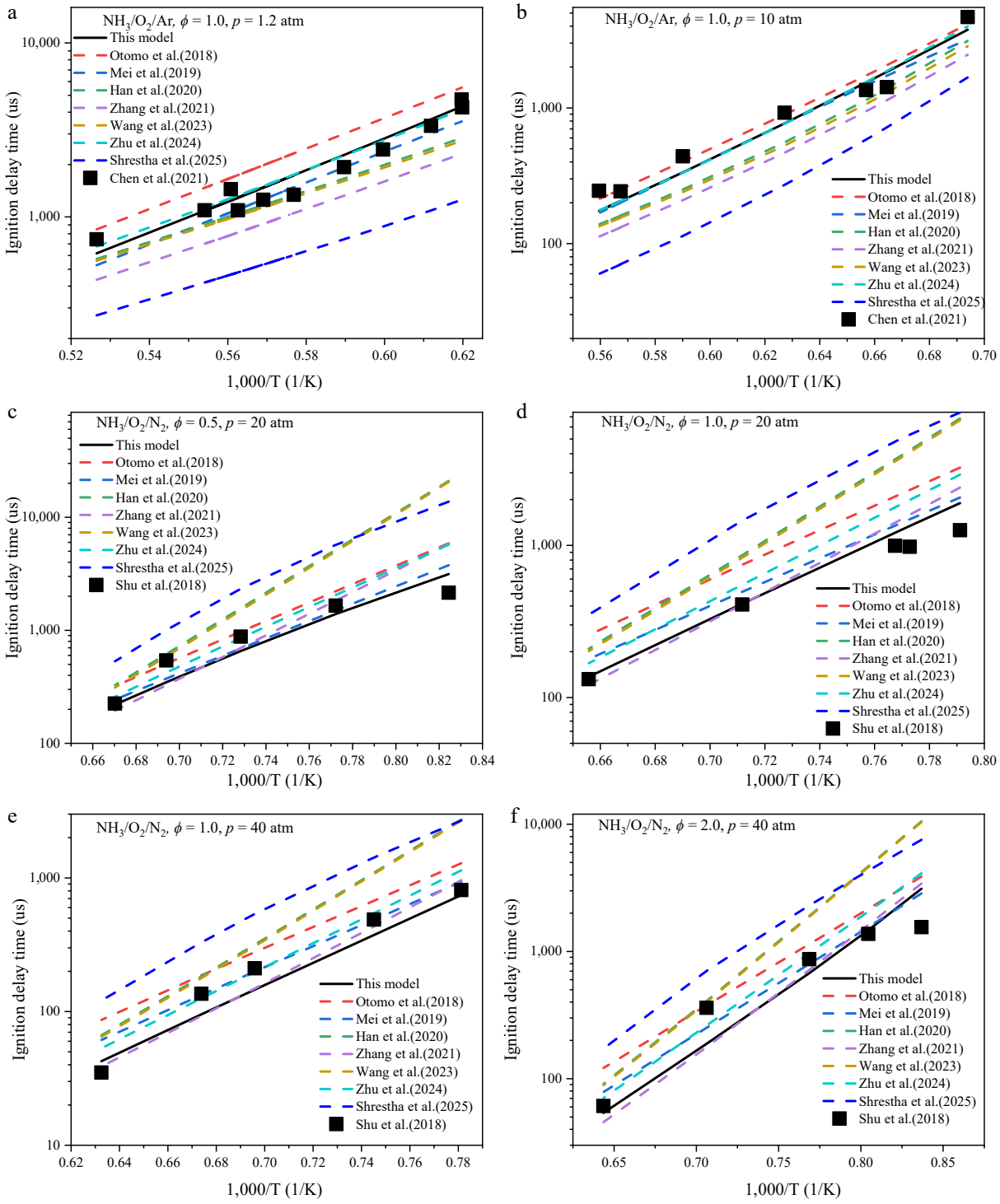

Fig. 9 Comparative verification of ignition delay time. (The lines represent predictions from the present model and the other seven models, while the symbols correspond to experimentally measured data reported in Shu et al.[22] and Chen et al.[25]).

the analysis of key species such as NH_3, H_2O, NO, and N_2 under lean-fuel environments. The model predictions for these species are validated against experimental data obtained from Dagaut et al.[27] and Osipova[29], as shown in Fig. 10. For other simulation conditions, refer to Supplementary File 1 (Fig. S8). The oxidation of NH_3 is mainly divided into three parts: the preparation stage at low temperatures (< 1,300 K), the rapid oxidation process at medium temperatures (< 1,370 K), and the slow oxidation and stabilization at high temperatures (> 1,370 K). In the research on components, the present model still shows good prediction performance. However, a limitation of this model is its tendency to underpredict the consumption rate of NH_3 and the formation rate of H_2O at intermediate temperatures, along with a slight underestimation of NO concentration. In comparison, several existing models exhibit faster prediction rates in this temperature regime. For instance, the models proposed by Otomo et al.[32] and Mei et al.[9] overpredict the rates of NH_3 consumption and H_2O generation compared to experimental values. Although the models developed by Zhang et al.[33] and Zhu et al.[37] demonstrate improved accuracy in predicting NO formation, they perform poorly in capturing NH_3 consumption and H_2O generation. The models by Han et al.[2] and Wang et al.[36] show relatively better performance in predicting NH_3 and H_2O profiles but tend to overpredict the formation rates of NO and N_2. The Shrestha model[34] predicts changes in NH_3 concentration relatively quickly overall, while also generating products such as H_2O and N_2 at a faster rate.

Kinetic analysis

Reaction path analysis

Fig. 11 depicts the primary reaction path analysis for ammonia combustion at a temperature of 1,600 K, a pressure of 1 atm, and an equivalence ratio (ϕ) of 1.0. The reaction pathways are analyzed using the nitrogen-element tracing method. Fifteen important reaction species and some reactions with an important reaction channel ratio greater than 1% are listed, Lysis reaction (LR). The results demonstrate that the primary reaction pathways identified by this model are in good agreement with those obtained from ReaxFF MD simulations. The formation of NH_2 from NH_3 mainly occurs through reactions R5, R24, and R25:

$$NH_3 + OH = NH_2 + H_2O \quad \text{(R24)}$$

$$NH_3 + O = NH_2 + OH \quad \text{(R25)}$$

Among them, R24 is dominant. The subsequent reactions of NH_2 can be divided into two parts: one is the process of generating N_2, and the other is the process of generating NO.

The process of generating N_2 can be divided into two main paths. One is $NH_2 \rightarrow$ (NH or $N_2H_4 \rightarrow N_2H_3 \rightarrow$) N_2H_2 (H_2NN) $\rightarrow$ NNH $\rightarrow N_2$,

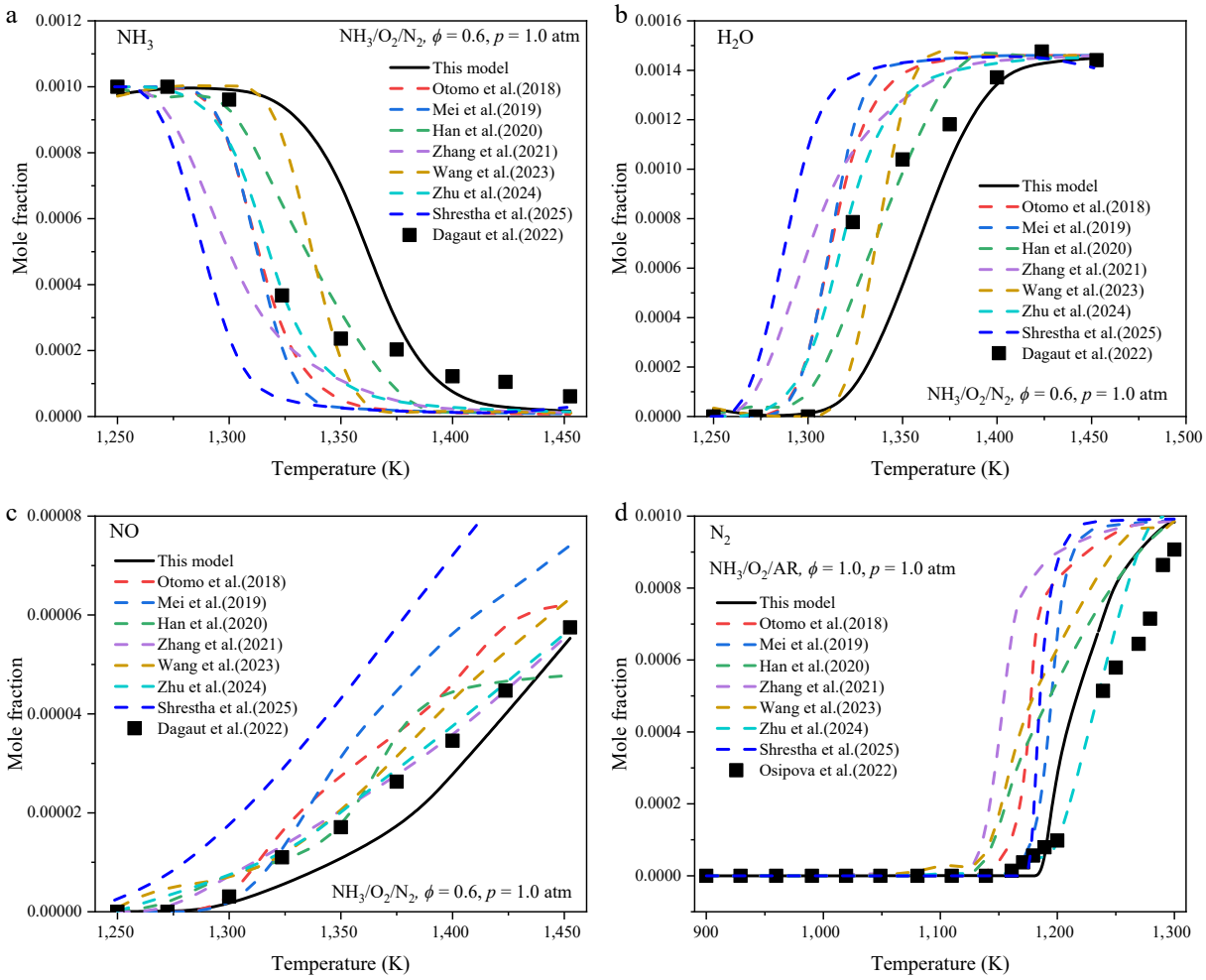

Fig. 10 Species concentration profiles comparison between present model (solid lines), seven reference models (dashed lines), and experimental measurements (symbols) from Dagaut et al.[27] and Osipova et al.[29].

and the other is $NH_2 \rightarrow NH \rightarrow N(NNH) \rightarrow N_2$. The first path is the primary one. In the first path, the formation of N_2H_4 from NH_2 can occur through reaction R26:

$$NH_2 + NH_2 + M = N_2H_4 + M \quad (R26)$$

N_2H_2 is generated indirectly. It can also be directly generated into N_2H_2 through reactions R27 and R28:

$$NH_2 + NH = N_2H_2 + H \quad (R27)$$

$$NH_2 + NH_2 = N_2H_2 + H_2 \quad (R28)$$

It is worth noting that in this process, both N_2H_4 and N_2H_3 are regarded as important substances and appear simultaneously in the reaction pathway in this model, which is consistent with the results of ReaxFF MD. However, in other models, these two substances are not simultaneously reflected as important substances in the main pathway. For example, the Otomo model[32], Mei model[9], and Zhang model[33] do not consider N_2H_4 as an important species, while the Wang model[36] does not include N_2H_3 as one of the 15 important species. The generation of N_2 from N_2H_2 mainly occurs through reactions R29–R35:

$$N_2H_2 + H = NNH + H_2 \quad (R29)$$

$$N_2H_2 + NH_2 = NH_3 + NNH \quad (R30)$$

$$N_2H_2 + M = NNH + H + M \quad (R31)$$

$$N_2H_2 + OH = NNH + H_2O \quad (R32)$$

$$N_2H_2 + O = NNH + OH \quad (R33)$$

$$NNH = H + N_2 \quad (R34)$$

$$NNH + O_2 = HO_2 + N_2 \quad (R35)$$

This pathway is dominant in the formation of N_2. Although the vast majority of H_2NN is converted into N_2, due to the relatively small amount of H_2NN generated from N_2H_3, the formation of N_2 from H_2NN is not the main pathway.

Similarly, the process of generating NO can also be divided into two main paths. One is $NH_2 \rightarrow NH$ or H_2NO and $HNOH \rightarrow HNO \rightarrow NO$, and the other is $NH_2 \rightarrow NH \rightarrow N \rightarrow NO$. The first path is the dominant one, and this path is basically consistent in the analysis of various models. In the main pathway of NO formation, H_2NO and HNOH, as isomers, can react with radicals such as NH_2, H, O, and OH to generate HNO, but H_2NO is dominant, which is consistent with the results of ReaxFF MD. The formation of NO from HNO mainly occurs through reactions R36–R41:

$$HNO + O_2 = NO + HO_2 \quad (R36)$$

$$HNO + NH = NH_2 + NO \quad (R37)$$

$$HNO + H = H_2 + NO \quad (R38)$$

$$HNO + O = NO + OH \quad (R39)$$

$$HNO = H + NO \quad (R40)$$

$$NH_2 + HNO = NH_3 + NO \quad (R41)$$

The generated NO can react with substances such as NH and N, enabling inter-conversion with NO. Although HNNO and H_2N_2O, which are involved in the formation of NO, are not shown in this reaction diagram, they are still important substances for NO formation. Moreover, when considering the main reaction pathways involving 20 important substances, HNNO is shown as one of the important substances.

The generated NO can react with substances such as NH and N to achieve mutual conversion with N_2. Although HNNO and H_2N_2O, which are involved in the formation of NO, are not shown in this reaction diagram, they are still important substances for NO formation. Moreover, when considering the main reaction pathways

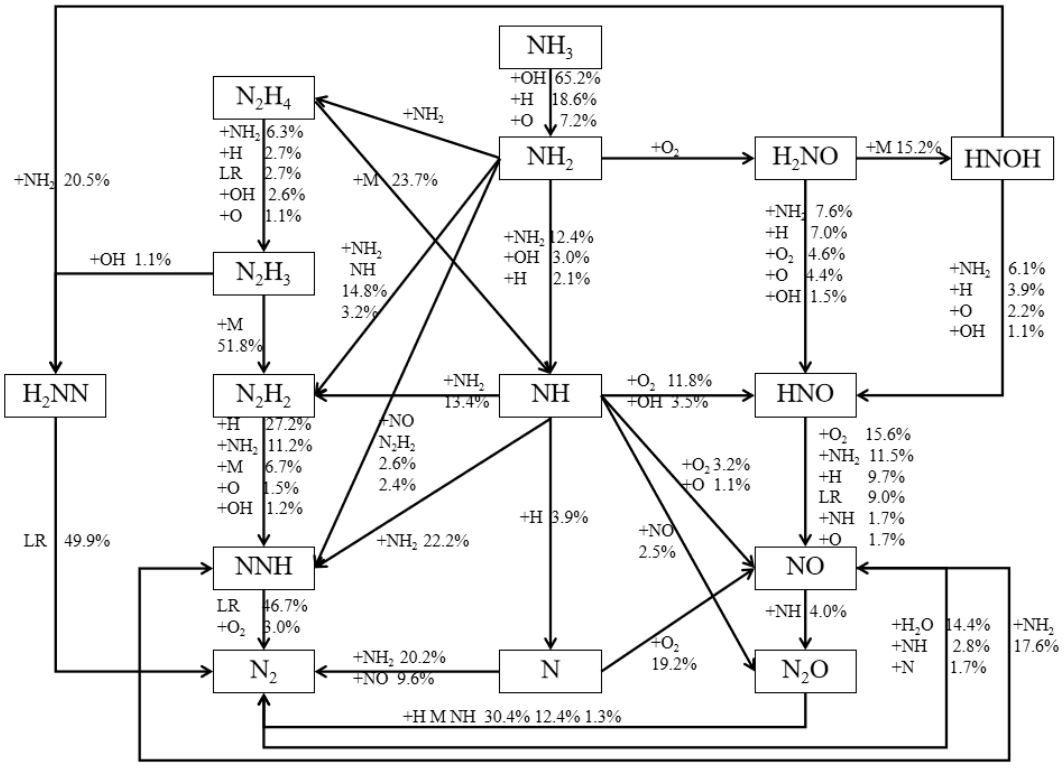

Fig. 11 The main reaction path of the ammonia combustion process.

involving 20 important substances, HNNO is shown as one of the important substances.

Sensitivity analysis

To investigate the key reactions influencing ammonia combustion characteristics, a comprehensive sensitivity analysis is conducted under various equivalence ratios, pressures, and temperatures. The results, presented in Fig. 12, include the effects of equivalence ratio on laminar burning velocity (LBV) and ignition delay time (IDT) across different pressure and temperature conditions, along with concentration profiles of major species such as NH_3, H_2O, and NO. A positive sensitivity coefficient indicates that the reaction promotes LBV, IDT, or species formation, whereas a negative value suggests an inhibitory effect.

In the LBV sensitivity analysis, the reaction $H + O_2 = O + OH$ exhibits the strongest promoting effect on ammonia LBV across all equivalence ratios, whereas the reaction $NH_2 + NO = N_2 + H_2O$ shows the greatest inhibitory influence. In addition, reactions such as $2OH = O + H_2O$, $NH_2 + OH = NH + H_2O$, $HNO = H + NO$, and $N_2O (+M) = N_2 + O (+M)$ are more sensitive under lean-fuel conditions. As the equivalence ratio increases, reactions such as $O + H_2 = OH + H$, $NH_2 + N = N_2 + 2H$, and $N_2H_2 + H = NNH + H_2$ gradually become more sensitive reactions. For IDT, as the equivalence ratio increases, the sensitive reactions basically remain unchanged; only the sensitivity coefficients change. Different from LBV, the reaction $NH_2 + HO_2 = H_2NO + OH$ replaces $H + O_2 = O + OH$ and becomes the most important reaction promoting IDT, while the reaction $NH_2 + NO = N_2 + H_2O$ is still the most important inhibitory reaction. Similarly, the study by Shrestha et al.[34] also found that the promoting reaction $H + O_2 = O + OH$ was not identified as a key reaction in enhancing NH_3 ignition, while the reaction $NH_2 + NO = N_2 + H_2O$ was observed to significantly inhibit the ignition characteristics of NH_3. The results of the sensitivity analysis of NH_3, H_2O, and NO show that the sensitive reactions of NH_3 and H_2O are completely the same. However, due to NH_3 being a reactant and H_2O being a product, the promoting or inhibitory effects of the sensitive reactions are completely opposite. The most important inhibitory reaction of NO is the same as that of H_2O. The difference is that $NH_2 + NO = N_2 + H_2O$ is the most important reaction promoting the formation of NO, and reactions related to NO formation, such as $NH_3 + O = NH_2 + OH$ and $NH + NO = N_2O + H$, gradually become more important.

It is worth noting that most of these sensitive reactions are related to NH_3, NH_2, and NH. Whether for LBV, IDT, or H_2O and NO (except NH_3), $NH_2 + NO = N_2 + H_2O$ is always the most important inhibitory reaction, and $H + O_2 = O + OH$ is a relatively important promoting reaction. At the same time, it was found that reactions such as $H + O_2 = O + OH$, $NH_2 + NO = N_2 + H_2O$, and $NH_2 + NO = NNH + OH$ are sensitive to any characteristic. The difference is that reactions such as $H + O_2 (+M) = HO_2 (+M)$ and $NH_2 + O = H + HNO$ (and reactions R3−1 to R3−9 in Supplementary File 1, Table S3) are mainly sensitive

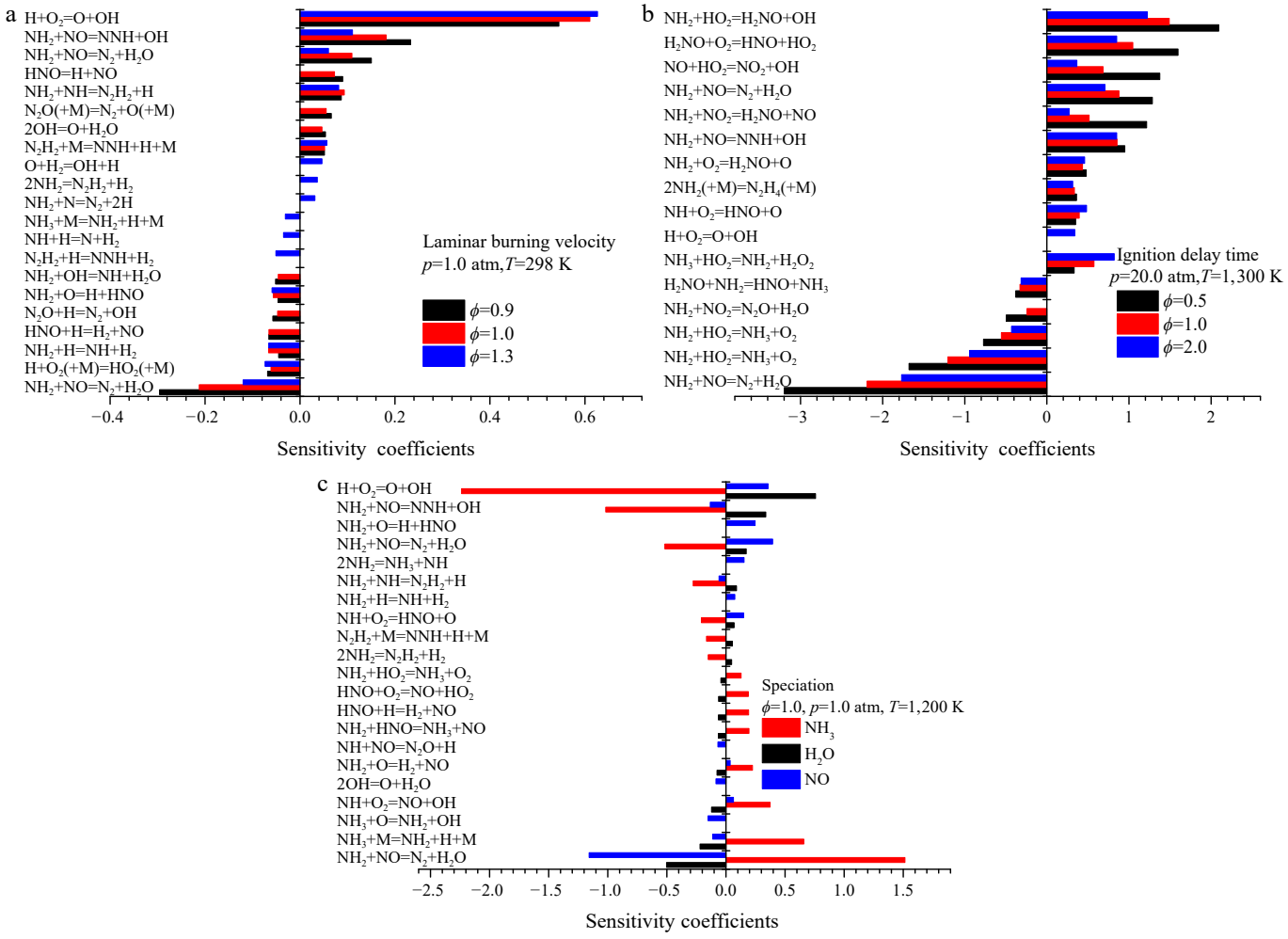

Fig. 12 Sensitivity analysis of laminar burning velocity, ignition delay time, and species.

to LBV, while reactions such as $NH_3 + HO_2 = NH_2 + H_2O_2$ and $NH_2 + HO_2 = H_2NO + OH$ (reactions R3−10 to R3−18 in Supplementary File 1, Table S3) are more sensitive to IDT, and $NH_3 + O = NH_2 + OH$ and $NH + NO = N_2O + H$ are only sensitive to NH_3, H_2O, and NO.

Additionally, the reaction mechanisms of key intermediates, including OH, NH_2, and NH, during ammonia reaction processes were examined based on rate of production (ROP) analysis. This analysis aims to elucidate the substantial influence of critical reactions on their formation and consumption, as depicted in Supplementary File 1 (Fig. S9). The production rate analysis reveals that reactions such as $O + H_2O = 2OH$, $H + O_2 = O + OH$, and $O + H_2 = OH + H$ play major roles in promoting OH generation, many of which involve O radicals. In contrast, reactions including $NH_3 + OH = H_2O + NH_2$, $OH + H_2 = H + H_2O$, and $NH_2 + OH = NH + H_2O$ contribute to OH consumption, often accompanied by the formation of H_2O. The primary reactions responsible for the formation of NH_2 and NH are $NH_3 + OH = NH_2 + H_2O$, $NH_2 + OH = NH + H_2O$, and $NH + OH = H + HNO$, indicating that reactions with OH not only serve as the main pathway for NH_3 consumption but also act as key channels for generating NH_2 and NH. The further consumption of NH_2 and NH also occurs via reactions with OH, such as $NH_2 + OH = NH + H_2O$ and $NH + OH = H + HNO$, underscoring the crucial role of OH in the ammonia combustion process.

Conclusions

Based on the ReaxFF MD simulation method, this paper methodically investigated the effects of varying equivalence ratios and temperatures on ammonia combustion behavior while elucidating the molecular-level reaction network and formation mechanisms of major products. By integrating newly identified ReaxFF MD-derived reaction pathways with existing mechanisms, a comprehensive ammonia combustion mechanism was developed. Furthermore, the model's combustion characteristics were extensively validated across diverse conditions. Key conclusions are summarized below:

(1) Variations in equivalence ratios (i.e., oxygen content) do not alter the reaction sequence of key radicals and products during ammonia combustion but significantly influence their quantitative yields. Elevated temperatures accelerate reaction kinetics, enhancing both the formation rates and peak concentrations of critical radicals and products.

(2) ReaxFF MD simulations reveal that NH_2 undergoes multiple reaction pathways, predominantly forming N_2 and NO. While isomers HNOH and H_2NO both contribute to HNO generation, H_2NO exhibits a dominant role. NO formation is primarily mediated by HNO, whereas N_2 production relies on NNH. Crucially, H_2N_2O and HNNO act as pivotal intermediates in NH_3 combustion, driving the conversion of NO to N_2 via the sequential pathway: $NO \rightarrow H_2N_2O \rightarrow HNNO \rightarrow N_2$.

(3) Employing a hierarchical construction approach, the critical reaction pathways in ammonia combustion were systematically identified through chemical kinetic analysis. By integrating ReaxFF MD simulations with combustion mechanism analysis, these reaction channels were rigorously validated and refined, culminating in a comprehensive ammonia combustion mechanism comprising 351 reactions and 41 species. Notably, the H_2N_2O species was incorporated into the ammonia kinetic mechanism for the first time as a pivotal pathway for NO formation. The mechanism was extensively validated across diverse operating conditions, including flame propagation speed, ignition delay time, and species concentration profiles. Results demonstrate strong predictive accuracy, confirming the model's robustness in capturing multi-target combustion characteristics.

(4) The mechanism reveals through path analysis that ammonia combustion reaction pathways are primarily categorized into two dominant routes: one governing N_2 formation and another involving NH_2 conversion to NO_x. The analytical results align closely with simulations obtained via the ReaxFF MD method. Sensitivity analysis further identifies that the majority of sensitive reactions are associated with species including NH_3, NH_2, NH, and H. Notably, Sensitivity analysis of laminar burning velocity (LBV), ignition delay time (IDT), and key species reveals that the inhibiting reaction $NH_2 + NO = N_2 + H_2O$ consistently dominates across these three combustion characteristics. The promoting reaction $H + O_2 = O + OH$ remains significantly influential on flame speed and the formation of major species, while its promoting effect on IDT becomes nearly negligible. Conversely, the reaction $NH_2 + HO_2 = H_2NO + OH$ exhibits the strongest promoting effect on IDT. Furthermore, NH_2-involved reactions that generate radicals such as OH and O, as well as those producing N_2 and H_2O, also contribute substantially to enhancing the ignition performance of ammonia.

This study effectively promotes the efficient application of NH_3. High-precision NH_3 combustion mechanism research reveals the unique nitrogen chemistry behavior of NH_3, particularly key intermediates and reaction pathways (e.g., $NH_2 + HO_2 = H_2NO + OH$, $NH_2 + NO = N_2 + H_2O$), deepening the understanding of nitrogen-containing fuel combustion mechanisms. In terms of model development, this study develops a high-precision kinetic model applicable over a wide range of conditions. It solves deviations in traditional mechanisms and offers a reliable foundation for simulating and predicting complex fuel systems like ammonia and its blends. This strongly supports the engineering application of low-carbon energy technologies.

Author contributions

The authors confirm contributions to the paper as follows: methodology: Li S, Wang K, Xi S; software: Li S, Wang K; investigation: Zhong L, Cao Z, Guo X, Hou J, Wen Z; validation: Guo X, Hou J; data curation: Cao Z, Wen Z; draft manuscript preparation: Li S, Wang K; writing – review and editing: Li S, Zhong L, Xi S; supervision: Li S, Wang K, Xi S; funding acquisition: Li S. All authors reviewed the results and approved the final version of the manuscript.

Data availability

All data generated or analyzed during this study are included in this published article and its supplementary information files.

Acknowledgments

This work was supported by the Natural Science Foundation of Henan (Grant Nos 242300420050, 252300420815), Henan Provincial Science and Technology Research Project (Grant Nos 252102220016, 252102221026, 252102220085), Henan Provincial Department of Education Science and Technology Research Key Project (Grant Nos 24A590006; 24B470010), and the Youth Research Funds Plan of Zhengzhou University of Aeronautics) (Grant Nos 24ZHQN01005, 25ZHQN01013), Special Project of the National Natural Science Foundation of China (Grant No. 62341125) and the program of the Innovation Research Team of Sci-tech, Henan Province (No. 25IRTSTHN020). Thanks to the ammonia/oxygen simulation model provided by Sichuan University.

Conflict of interest

The authors declare that all individuals involved in this work are listed as co-authors, and the cooperation between the authors is not a paid collaboration, with no potential conflicts of interest. There are no other known competing financial interests or personal relationships that could have influenced the work reported in this paper. Although author Kunqi Wang is an employee of AECC Chengdu Engine Co., Ltd., the work presented herein is independent academic research and is not related to the commercial interests of the company. The author declares that no financial or other contractual agreements between the company and the authors or their institutions influenced the design, outcome, or reporting of this study.

Supplementary information accompanies this paper online at: https://doi.org/10.48130/prkm-0026-0006.

Dates

Received 23 June 2025; Revised 6 December 2025; Accepted 24 February 2026; Published online 30 May 2026

References

[1] Kobayashi H, Hayakawa A, Somarathne KA, Okafor EC. 2019. Science and technology of ammonia combustion. *Proceedings of the Combustion Institute* 37(1):109–133

[2] Han X, Wang Z, He Y, Zhu Y, Cen K. 2020. Experimental and kinetic modeling study of laminar burning velocities of NH_3/syngas/air premixed flames. *Combustion and Flame* 213:1–13

[3] Reiter AJ, Kong SC. 2011. Combustion and emissions characteristics of compression-ignition engine using dual ammonia-diesel fuel. *Fuel* 90(1):87–97

[4] Pacheco GP, Rocha RC, Franco MC, Mendes MAA, Fernandes EC, et al. 2021. Experimental and kinetic investigation of stoichiometric to rich NH_3/H_2/air flames in a swirl and bluff-body stabilized burner. *Energy & Fuels* 35(9):7201–7216

[5] Tang G, Jin P, Bao Y, Chai WS, Zhou L. 2021. Experimental investigation of premixed combustion limits of hydrogen and methane additives in ammonia. *International Journal of Hydrogen Energy* 46(39):20765–20776

[6] Kim HK, Ku JW, Ahn YJ, Kim YH, Kwon OC. 2021. Effects of O_2 enrichment on NH_3/air flame propagation and emissions. *International Journal of Hydrogen Energy* 46(46):23916–23926

[7] Chen DN, Li J, Huang HY, Chen Y, He ZH, et al. 2020. Progress on ammonia combustion and reaction mechanism. *Chemistry* 83(6):508–515 (in Chinese)

[8] Takizawa K, Takahashi A, Tokuhashi K, Kondo S, Sekiya A. 2008. Burning velocity measurements of nitrogen-containing compounds. *Journal of Hazardous Materials* 155(1–2):144–152

[9] Mei B, Zhang X, Ma S, Cui M, Guo H, et al. 2019. Experimental and kinetic modeling investigation on the laminar flame propagation of ammonia under oxygen enrichment and elevated pressure conditions. *Combustion and Flame* 210:236–246

[10] Lhuillier C, Brequigny P, Lamoureux N, Contino F, Mounaïm-Rousselle C. 2020. Experimental investigation on laminar burning velocities of ammonia/hydrogen/air mixtures at elevated temperatures. *Fuel* 263:116653

[11] Hayakawa A, Goto T, Mimoto R, Arakawa Y, Kudo T, et al. 2015. Laminar burning velocity and Markstein length of ammonia/air premixed flames at various pressures. *Fuel* 159:98–106

[12] Chen X, Liu Q, Jing Q, Mou Z, Shen Y, et al. 2021. Flame front evolution and laminar flame parameter evaluation of buoyancy-affected ammonia/air flames. *International Journal of Hydrogen Energy* 46(77):38504–38518

[13] Shrestha KP, Lhuillier C, Barbosa AA, Brequigny P, Contino F, et al. 2021. An experimental and modeling study of ammonia with enriched oxygen content and ammonia/hydrogen laminar flame speed at elevated pressure and temperature. *Proceedings of the Combustion Institute* 38(2):2163–2174

[14] Kanoshima R, Hayakawa A, Kudo T, Okafor EC, Colson S, et al. 2022. Effects of initial mixture temperature and pressure on laminar burning velocity and Markstein length of ammonia/air premixed laminar flames. *Fuel* 310:122149

[15] Liang B, Gao W, Zhang K, Li Y. 2023. Ammonia-air combustion and explosion characteristics at elevated temperature and elevated pressure. *International Journal of Hydrogen Energy* 48(53):20225–20237

[16] Alvarez LF, Shaffer J, Dumitrescu CE, Askari O. 2024. Laminar burning velocity of Ammonia/Air mixtures at high pressures. *Fuel* 363:130986

[17] Zhou S, Cui B, Yang W, Tan H, Wang J, et al. 2023. An experimental and kinetic modeling study on NH_3/air, NH_3/H_2/air, NH_3/CO/air, and NH_3/CH_4/air premixed laminar flames at elevated temperature. *Combustion and Flame* 248:112536

[18] Kohansal M, Kiani M, Masoumi S, Nourinejad S, Ashjaee M, et al. 2023. Experimental and numerical investigation of NH_3/CH_4 mixture combustion properties under elevated initial pressure and temperature. *Energy & Fuels* 37(14):10681–10696

[19] Liu B, Hu E, Yin G, Huang Z. 2023. Experimental and kinetic study on laminar burning velocities of ammonia/ethylene/air premixed flames under high temperature and elevated pressure. *Combustion and Flame* 251:112707

[20] Hu E, Li X, Meng X, Chen Y, Cheng Y, et al. 2015. Laminar flame speeds and ignition delay times of methane–air mixtures at elevated temperatures and pressures. *Fuel* 158:1–10

[21] Mathieu O, Petersen EL. 2015. Experimental and modeling study on the high-temperature oxidation of Ammonia and related NO_x chemistry. *Combustion and Flame* 162(3):554–570

[22] Shu B, Vallabhuni SK, He X, Issayev G, Moshammer K, et al. 2019. A shock tube and modeling study on the autoignition properties of ammonia at intermediate temperatures. *Proceedings of the Combustion Institute* 37(1):205–211

[23] He X, Shu B, Nascimento D, Moshammer K, Costa M, et al. 2019. Autoignition kinetics of ammonia and ammonia/hydrogen mixtures at intermediate temperatures and high pressures. *Combustion and Flame* 206:189–200

[24] Dai L, Gersen S, Glarborg P, Levinsky H, Mokhov A. 2020. Experimental and numerical analysis of the autoignition behavior of NH_3 and NH_3/H_2 mixtures at high pressure. *Combustion and Flame* 215:134–144

[25] Chen J, Jiang X, Qin X, Huang Z. 2021. Effect of hydrogen blending on the high temperature auto-ignition of ammonia at elevated pressure. *Fuel* 287:119563

[26] Peng Y, Ranjan D, Sun W. 2023. A shock tube study of fuel concentration effect on high-pressure autoignition delay of ammonia. *Applications in Energy and Combustion Science* 16:100202

[27] Dagaut P. 2022. On the oxidation of ammonia and mutual sensitization of the oxidation of No and ammonia: experimental and kinetic modeling. *Combustion Science and Technology* 194(1):117–129

[28] Manna MV, Sabia P, Ragucci R, de Joannon M. 2020. Oxidation and pyrolysis of ammonia mixtures in model reactors. *Fuel* 264:116768

[29] Osipova KN, Zhang X, Sarathy SM, Korobeinichev OP, Shmakov AG. 2022. Ammonia and ammonia/hydrogen blends oxidation in a jet-stirred reactor: experimental and numerical study. *Fuel* 310:122202

[30] Sabia P, Manna MV, Cavaliere A, Ragucci R, de Joannon M. 2020. Ammonia oxidation features in a Jet Stirred Flow Reactor. The role of NH2 chemistry. *Fuel* 276:118054

[31] Song Y, Hashemi H, Christensen JM, Zou C, Marshall P, et al. 2016. Ammonia oxidation at high pressure and intermediate temperatures. *Fuel* 181:358–365

[32] Otomo J, Koshi M, Mitsumori T, Iwasaki H, Yamada K. 2018. Chemical kinetic modeling of ammonia oxidation with improved reaction mechanism for ammonia/air and ammonia/hydrogen/air combustion. *International Journal of Hydrogen Energy* 43(5):3004–3014

[33] Zhang X, Moosakutty SP, Rajan RP, Younes M, Sarathy SM. 2021. Combustion chemistry of ammonia/hydrogen mixtures: jet-stirred reactor measurements and comprehensive kinetic modeling. *Combustion and Flame* 234:111653

[34] Shrestha KP, Giri BR, Pelé R, Aljohani K, Brequigny P, et al. 2025. A comprehensive chemical kinetic modeling and experimental study of NH_3–methanol/ethanol combustion towards net-zero CO_2 emissions. *Combustion and Flame* 274:113954

[35] Bertolino A, Fürst M, Stagni A, Frassoldati A, Pelucchi M, et al. 2021. An evolutionary, data-driven approach for mechanism optimization: theory and application to ammonia combustion. *Combustion and Flame* 229:111366

[36] Wang Z, Ji C, Zhang T, Wang D, Zhai Y, et al. 2023. Experimental and numerical study on laminar premixed $NH_3/H_2/O_2$/air flames. *International Journal of Hydrogen Energy* 48(39):14885–14895

[37] Zhu Y, Curran HJ, Girhe S, Murakami Y, Pitsch H, et al. 2024. The combustion chemistry of ammonia and ammonia/hydrogen mixtures: a comprehensive chemical kinetic modeling study. *Combustion and Flame* 260:113239

[38] Zhang Y, Cui LM, Niu T, Hong DK. 2024. Study on the synergistic mechanism of co-pyrolysis of coal and ammonia based on ReaxFF molecular dynamics method. *Journal of Engineering for Thermal Energy and Power* 39(6):98–106 (in Chinese)

[39] Huang FQ, Wang J, Jiang XZ. 2023. Reactive molecular dynamics of the effect of H_2 on the combustion of NH_3 in air. *Advances in New and Renewable Energy* 11(5):404–410 (in Chinese)

[40] Zhang Q, Guo L, Cai X, Shan S, Li K, et al. 2021. Chemical effect of CH_4 on NH_3 combustion in an O_2/N_2 environment *via* ReaxFF. *Energy & Fuels* 35(13):10918–10928

[41] Hong D, Yuan L, Wang C. 2022. Competition between NH_3-O_2 reaction and char-O_2 reaction and its influence on NO generation and reduction during char/NH_3 co-combustion: reactive molecular dynamic simulations. *Fuel* 324:124666

[42] Guo Y, Shi H, Liu H, Xie Y, Guan Y. 2023. Reactive molecular dynamics simulation and chemical kinetic modeling of ammonia/methane co-combustion. *Fuel* 354:129341

[43] Wang J, Jiang XZ, Luo KH. 2023. Exploring reaction mechanism for ammonia/methane combustion *via* reactive molecular dynamics simulations. *Fuel* 331:125806

[44] Hong D, Yuan L, Wang C. 2024. The influence of NH_3 on coal combustion kinetics during coal/NH_3 cocombustion: experiments and ReaxFF MD simulations. *Energy & Fuels* 38(10):9120–9129

[45] Wang Y, Sun J, Liu Q, Chen L, Gu M, et al. 2024. NO_x formation mechanism of plasma assisted ammonia combustion: a reactive molecular dynamics study. *Energy* 293(C):130706

[46] van Duin ACT, Dasgupta S, Lorant F, Goddard WA. 2001. ReaxFF: a reactive force field for hydrocarbons. *The Journal of Physical Chemistry A* 105(41):9396–9409

[47] Senftle TP, Hong S, Islam MM, Kylasa SB, Zheng Y, et al. 2016. The ReaxFF reactive force-field: development, applications and future directions. *npj Computational Materials* 2:15011

[48] Aktulga HM, Fogarty JC, Pandit SA, Grama AY. 2012. Parallel reactive molecular dynamics: numerical methods and algorithmic techniques. *Parallel Computing* 38(4–5):245–259

[49] Stukowski A. 2010. Visualization and analysis of atomistic simulation data with OVITO–the Open Visualization Tool. *Modelling and Simulation in Materials Science and Engineering* 18(1):015012

[50] Liu Q, Huang W, Liu B, Wang PC, Chen HB. 2021. Gamma radiation chemistry of polydimethylsiloxane foam in radiation-thermal environments: experiments and simulations. *ACS Applied Materials & Interfaces* 13(34):41287–41302

[51] Zhang L, van Duin ACT, Zybin SV, Goddard WA, III. 2009. Thermal decomposition of hydrazines from reactive dynamics using the ReaxFF reactive force field. *The Journal of Physical Chemistry B* 113(31):10770–10778

[52] Goodwin DG, Speth RL, Moffat HK, Weber BW. 2018. *Cantera: an object-oriented software toolkit for chemical kinetics, thermodynamics, and transport processes*. Version 2.4.0 ed. doi: 10.5281/zenodo.742000

[53] Hashemi H, Christensen JM, Gersen S, Glarborg P. 2015. Hydrogen oxidation at high pressure and intermediate temperatures: experiments and kinetic modeling. *Proceedings of the Combustion Institute* 35(1):553–560

[54] Meng Q, Lei L, Lee J, Burke MP. 2023. On the role of HNNO in NO_x formation. *Proceedings of the Combustion Institute* 39(1):551–560

[55] National Institute of Standards and Technology. 2026. *Kinetics database*. https://kinetics.nist.gov

[56] Miller JA, Klippenstein SJ. 2000. Theoretical considerations in the NH_2 + NO reaction. *The Journal of Physical Chemistry A* 104(10):2061–2069

[57] Yokoyama K, Sakane Y, Fueno T. 1991. Formations of OH($X^2\Pi$, $A^2\Sigma^+$) in the reaction of NH($^3\Sigma^-$) with NO in incident shock waves. *Bulletin of the Chemical Society of Japan* 64(6):1738–1742

[58] Li Y, Bi M, Li B, Gao W. 2018. Explosion behaviors of ammonia–air mixtures. *Combustion Science and Technology* 190(10):1804–1816